novel monoclonal antibody, SM/C-2.6, has recently been established (23). Satellite cells purified with this antibody regenerate muscle fibers on implantation into mdx mice (15).

The use of satellite cells for clinical therapies would require the establishment of a reliable source of these cells. Embryonic stem (ES) cells are totipotent stem cells that are able to differentiate into various types of somatic cells *in vitro*. While mouse embryonic stem (mES) cells can be readily induced to differentiate into muscle fibers (24, 25) and the myogenicity of human ES cells was recently validated (26), the induction of mES cells into functional satellite cells has not been reported. Here we have successfully induced mES cells to generate cells expressing Pax7 *in vitro* by forming embryoid bodies (EBs). These ES cell-derived (ES-derived) Pax7-positive cells can be enriched using the SM/C-2.6 antibody (23) and possess a great potential for generating mature skeletal muscle fibers both *in vitro* and *in vivo*. The Pax7-positive cells display a self-renewal ability that can repopulate Pax7-positive cells *in vivo* in the recipient muscles following an injury. Furthermore, these ES-derived Pax7-positive cells could engraft in the recipient muscle for long periods, up to 24 wk, and could also be serially transplanted. These results indicate that ES-derived Pax7-positive cells possess satellite cell characteristics. This is the first report of effective induction of functional satellite cells from mES cells, and these novel findings may provide a new therapeutic approach for treatment of DMD.

MATERIALS AND METHODS

Cell culture

D3 cells, mES cells (27) that ubiquitously express the *EGFP* gene under the *CAG* promoter (28) (a gift from Dr. Masaru Okabe, Osaka University, Osaka, Japan), were used in this study. ES cells were maintained on tissue culture dishes (Falcon) coated with 0.1% gelatin (Sigma, Oakville, CA, USA), in DMEM (Sigma) supplemented with 15% fetal bovine serum (FBS; Thermo Trace, Melbourne, Australia), 0.1 mM 2-mercaptoethanol (Nakalai Tesque, Japan), 0.1 mM nonessential amino acids (Invitrogen, Burlington, CA, USA), 1 mM sodium pyruvate (Sigma), penicillin/streptomycin (50 μg/mL), and 5000 U/ml leukemia inhibitory factor (Dainippon Pharmaceutical Co., Japan).

In vitro differentiation of ES cells into a muscle lineage

To induce EB formation, undifferentiated ES cells were cultured in hanging drops for 3 d at a density of 800 cells/20 μl of differentiation medium, which consisted of DMEM supplemented with penicillin/streptomycin, 0.1 mM nonessential amino acids, 0.1 mM 2-mercaptonethanol, 5% horse serum (HS), and 10% FBS. EBs were transferred to suspension cultures for an additional 3 d (d 3+3). Finally, the EBs were plated in differentiation medium in 48-well plates (Falcon) coated with Matrigel (BD Bioscience, Bedford, MA, USA). The medium was changed every 5 d.

Immunofluorescence and immunocytochemical analysis

Immunostaining of cultured cells and recipient mouse tissues were carried out as described previously (29). Briefly, the left tibialis anterior (LTA) muscle of the recipient mouse was fixed with 4% paraformaldehyde and cut into 6 μm cross sections using a cryostat, and samples were fixed for 5 min in 4% paraformaldehyde (PFA) in PBS and permeabilized with 0.1% Triton X-100 in PBS for 10 min. After incubation in 5% skim milk for 10 min at room temperature to block nonspecific antibody binding, cells were incubated for 12 h at 4°C with anti-mouse monoclonal antibodies. Antibodies used in this study were mouse anti-Pax7, which was biotinylated using a DSB-X Biotin Protein Labeling Kit (D20655; Molecular Probes, Eugene, OR, USA), mouse anti-Pax3 (MAB1675, MAB2457; R&D Systems, Minneapolis, MN, USA), rabbit anti-mouse Myf5 (sc-302; Santa Cruz Biotechnology, Santa Cruz, CA, USA), mouse anti-mouse M-cadherin (205610; Calbiochem, San Diego, CA, USA), mouse anti-myosin heavy chain (MHC; 18-0105; Zymed Laboratories, San Francisco, CA, USA; reacts with human, rabbit, rat, mouse, bovine, and pig skeletal MHC), mouse anti-mouse myogenin and mouse anti-mouse Myo-D1 (M3559, M3512; Dako, Carpinteria, CA, USA), monoclonal rabbit anti-mouse laminin (LB-1013; LSL, Tokyo, Japan), and mouse anti-mouse dystrophin (NCL-DYS2; Novocastra Laboratories, Newcastle-upon-Tyne, UK). Cy3-labeled antibodies to mouse or rabbit IgG, fluorescein isothiocyanate-labeled antibodies to mouse or rabbit IgG (715-005-150, 711-165-152; Jackson ImmunoResearch Laboratory, Bar Harbor, ME, USA), or Alexa 633-labeled goat anti-rabbit IgG (A21070; Invitrogen, Molecular Probes) were applied as secondary antibodies. Hoechst 33324 (H3570; Molecular Probes) was used for nuclear staining. The samples were examined with a fluorescence microscope (Olympus, Tokyo, Japan) or an AS-MDW system (Leica Microsystems, Wetzlar, Germany). Micrographs were obtained using an AxioCam (Carl Zeiss Vision, Hallbergmoos, Germany) or the AS-MDW system (Leica Microsystems). In sections of muscles transplanted with ES-derived satellite cells, the number of GFP-positive muscle fascicles and GFP/Pax7-double-positive cells were counted, per field, at ×100. More than 10 fields in each tissue sample were observed. To prevent nonspecific secondary antibody binding to Fc receptors, all immunostaining of frozen sections used the Vector® M.O.M™ Immunodetection Kit (BMK-2202; Vector Laboratories, Burlingame, CA, USA).

PCR analysis

Total RNA was isolated from cultured cells in 48-well plates, using TRIzol reagent (Invitrogen). The following specific primers were used for PCR:

Pax3, sense, 5′-AACACTGGCCCTCAGTGAGTTCTAT-3′, and antisense, 5′-ACTCAGGATGCCATCGATGCTGTG-3′; Pax7, sense, 5′-CATCCAGTGCTGGTACCCCACAG-3′, and antisense, 5′-CTGTGGATGTCACCTGCTTGAA-3′; Myf5, sense, 5′-GAGCTGCTGAGGGAACAGGTGG-3′, and antisense, 5′-GTTCTTTCGGGACCAGACAGGG-3′; MyoD, sense, 5′-AGGCTCTGCTGCGCGACCAG-3′, and antisense, 5′-TGCAGTCGATCTCTCAAAGC-3′; myogenin, sense, 5′-TGAGGGAGAAGCGCAGGCTCAAG-3′, and antisense, 5′-ATGCTGTCCACGATGGACGTAAGG-3′; M-cadherin, sense, 5′-CCACAAACGCCTCCCCTACCC-3′, and antisense, 5′-GTCGATGCTGAAGAACTCAGGGC-3′; C-met, sense, 5′-GAATGTCGTCCTACACGGCCAT-3′, and antisense, 5′-CACTACACAGTCAGGACACTGC-3′; GAPDH, sense, 5′-TGAAGGTCGGTGTGAACGGATTTGGC-3′, and antisense, 5′-TGTTGGGGGCCGAGTTGGGATA-3′. AmpliTaqGold (Applied

Biosystems, Foster City, CA, USA) was used for PCR amplification. The amplification program used was 35 cycles of 30 s at 94°C, 30 s at 64°C, and 40 s at 72°C, with a final incubation of 7 min at 72°C.

Flow cytometry and cell sorting

Cultured cells were incubated with enzyme-free Hank's-based Cell Dissociation Buffer (Invitrogen) for 30 min at 37°C and gently dissociated into single cells. The cells were then washed with PBS twice, probed with biotinylated-SM/C-2.6 (23) antibody for 15 min at room temperature, and stained with phycoerythrin-conjugated strepavidin (12-4312; eBioscience, San Diego, CA, USA) for 15 min at room temperature. Dead cells were excluded from the plots based on propidium iodide staining (Sigma), and SM/C-2.6-positive cells were collected using a FACS Vantage instrument (Becton Dickinson, San Jose, CA, USA). Sorted cells were plated (1×10^4 cells/well) with differentiation medium in 96-well plates (Falcon) coated with Matrigel (008504; BD Bioscience). The medium was changed every 5 d, and 7 d after plating the cultured cells were analyzed.

Intramuscular cell transplantation (primary transplantation)

Recipient mice were injected with 50 μl of 10 μM cardiotoxin (CTX; Latoxan, Valence, France) (30) in the LTA muscle 24 h before transplantation (31). CTX is a myotoxin that destroys myofibers, but not satellite cells, and leaves the basal lamina and microcirculation intact. Since proliferation of host myogenic cells may prevent the incorporation of transplanted cells, recipient mdx mice (15) received 8 cGy of systemic irradiation (32) 12 h before transplantation to block muscle repair by endogenous cells. An average of 4.53×10^4 ES-derived SM/C-2.6-positive or -negative cells were washed twice with 500 μl of PBS, resuspended in 20 μl of DMEM, and injected into the LTA muscle of recipient mdx mice using an allergy syringe (Becton Dickinson). Mdx mice, which are derived from the CL/B16 strain, were used as the recipient mice in all experiments. Similarly, D3 ES cells, which are derived from the 129X1/SvJ ES cells, were used in all experiments. The major histocompatibility complex (MHC) of mdx mouse and D3 cells are very similar, both possessing type *b* MHC H2 haplotypes. All animal-handling procedures followed the Guild for the Care and Use of Laboratory Animals published by the U.S. National Institutes of Health (NIH Publication No. 85-23, revised 1996) and the Guidelines of the Animal Research Committee of the Graduate School of Medicine, Kyoto University.

Secondary transplantation

The LTA muscles of recipient mice were collected 8 wk after the primary transplantation. The muscles were minced and digested into single cells with 0.5% collagenase type I (lot S4D7301; Worthington Biochemical Corp., Lakewood, NJ, USA). After washing with PBS and filtration through a 100 μm filter, Pax7-positive cells were sorted by FACS using the SM/C-2.6 antibody. SM/C-2.6-positive cells (200 cells/mouse) were injected into preinjured LTA muscles of secondary recipient mice. The LTA muscles were analyzed 8 wk after transplantation.

Isolation and immunostaining of single fibers

To detect muscle satellite cells attaching to single fibers with Pax7, muscle fibers from the LTA muscle of recipient mice were prepared essentially according to the method of Bischoff in Rosenblatt *et al.* (33). Briefly, dissected muscles were incubated in DMEM containing 0.5% type I collagenase (Worthington) at 37°C for 90 min. The tissue was then transferred to prewarmed DMEM containing 10% FBS. The tissue was gently dissociated into single fibers by trituration with a fire-polished wide-mouth Pasteur pipette. Fibers were transferred to a Matrigel-coated 60 mm culture dish (Falcon) and fixed in 4% PFA for 5 min at room temperature. Fibers were permeabilized with 0.1% Triton X-100 in PBS for 10 min, and nonspecific binding was blocked by incubation in 5% skim milk for 10 min at room temperature. Primary mouse monoclonal antibodies against mouse Pax7 were applied for 12 h at 4°C. Antibodies were detected using the secondary antibodies described above.

Statistics

Data are presented as means ± SD. For comparison of the numbers of MHC and Pax7-positive cells in the sorted SM/C-2.6-positive and -negative fractions and the numbers of GFP-positive muscle fascicles and GFP/Pax7-double-positive cells in reinjured and noninjured groups, the unpaired Student's *t* test was used, and a value of $P < 0.05$ was considered to be statistically significant.

RESULTS

Myogenic lineage cells are effectively induced from mES cells *in vitro*

EBs were formed in hanging drop cultures for 3 d followed by an additional 3 d in suspension cultures (Fig. 1*A*). These EBs were then plated onto Matrigel-coated 48-well plates in differentiation medium, which contained 5% HS. This culture method is a modified version of the classical ES cell differentiation method (25) and the skeletal muscle single fiber culture method (33). After plating, EBs quickly attached to the bottom of the coated dishes, and spindle-shaped fibers appeared surrounding the EBs by the seventh day of plating (d 3+3+7; Fig. 1*B*). As these spindle fibers grew, they began to fuse with each other, forming thick multinucleated fibers resembling skeletal myofibers (Fig. 1*C, D*). At the same time we observed spontaneous contractions by the fibers (Supplemental Videos 1 and 2), a trait commonly seen in cultured skeletal muscle fibers. Immunostaining showed that these fused fibers were positive for skeletal-muscle-specific MHC (Fig. 1*E*). Furthermore, cells expressing muscle regulatory factor (MRF) proteins, including Pax7 (Fig. 1*F*), Myf5 (Fig. 1*G*), MyoD (Fig. 1*H*), and myogenin (Fig. 1*I*) were observed. On d 3 + 3 + 14, the average number of MHC-positive wells was 73.6 ± 5.8% (n=144). In all the MHC-positive wells, cells expressing Pax7, an essential transcription factor in satellite cells, were also observed. Double staining for Pax7 and MyoD confirmed the existence of cells staining for Pax7 alone, indicating the presence of quiescent-state satellite cells (34) within the culture (Supplemental Fig. 1). Next, the time course of MRF expression was examined by RT-PCR (Fig. 1*J*). Expression of Pax3 and Pax7 both peaked on d 3 + 3 +

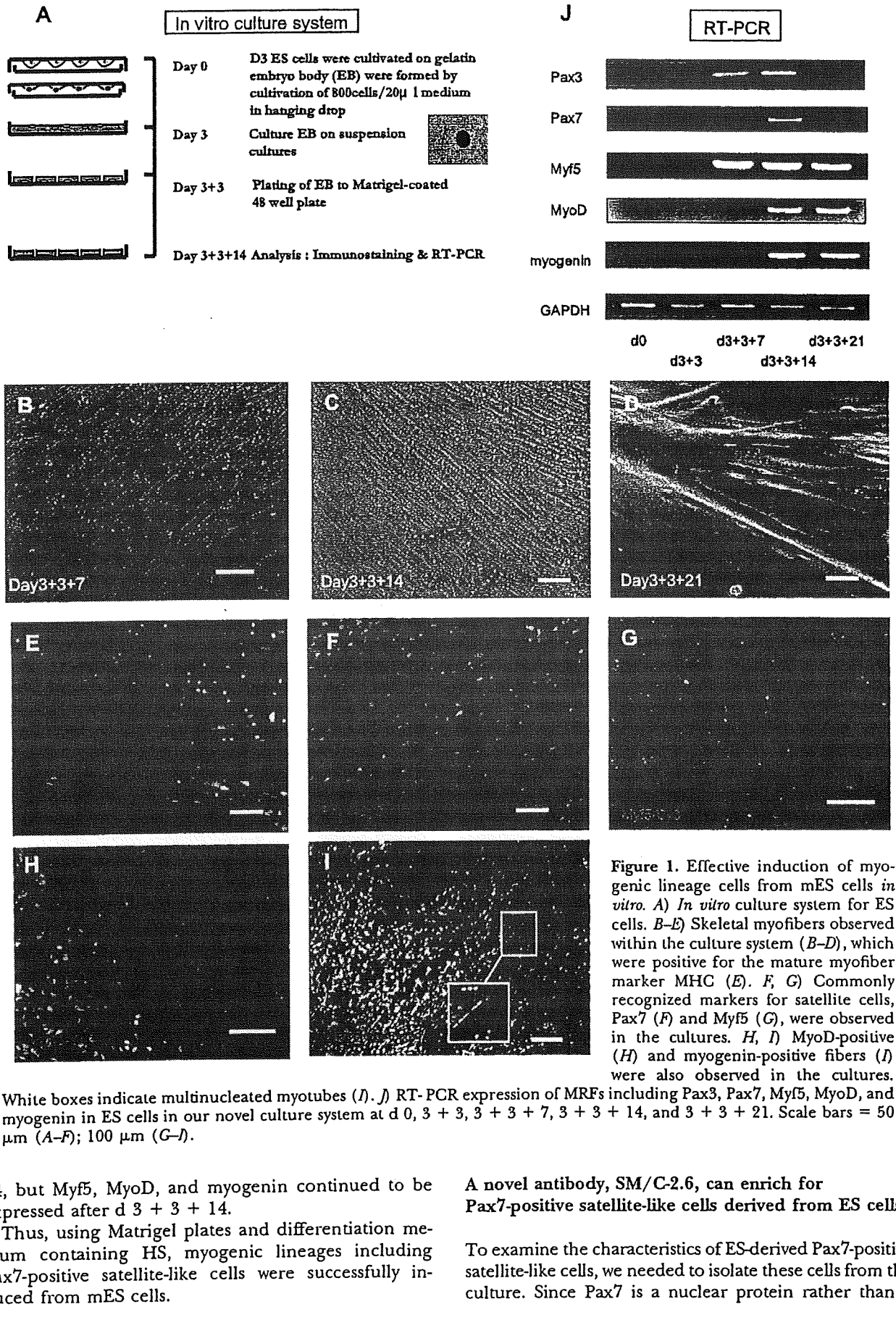

Figure 1. Effective induction of myogenic lineage cells from mES cells *in vitro*. *A*) *In vitro* culture system for ES cells. *B–E*) Skeletal myofibers observed within the culture system (*B–D*), which were positive for the mature myofiber marker MHC (*E*). *F, G*) Commonly recognized markers for satellite cells, Pax7 (*F*) and Myf5 (*G*), were observed in the cultures. *H, I*) MyoD-positive (*H*) and myogenin-positive fibers (*I*) were also observed in the cultures. White boxes indicate multinucleated myotubes (*I*). *J*) RT-PCR expression of MRFs including Pax3, Pax7, Myf5, MyoD, and myogenin in ES cells in our novel culture system at d 0, 3 + 3, 3 + 3 + 7, 3 + 3 + 14, and 3 + 3 + 21. Scale bars = 50 μm (*A–F*); 100 μm (*G–I*).

14, but Myf5, MyoD, and myogenin continued to be expressed after d 3 + 3 + 14.

Thus, using Matrigel plates and differentiation medium containing HS, myogenic lineages including Pax7-positive satellite-like cells were successfully induced from mES cells.

A novel antibody, SM/C-2.6, can enrich for Pax7-positive satellite-like cells derived from ES cells

To examine the characteristics of ES-derived Pax7-positive satellite-like cells, we needed to isolate these cells from the culture. Since Pax7 is a nuclear protein rather than a

surface marker, anti-Pax7 antibodies cannot be used for living cell separation by FACS. Therefore, a novel antibody, SM/C-2.6 (23), was used to detect satellite cells. SM/C-2.6 detects quiescent adult mouse satellite cells, as well as satellite cells in neonatal muscle tissue, as determined by immunostaining (Supplemental Fig. 2). RT-PCR confirmed that sorted SM/C-2.6-positive cells expressed Pax3, Pax7, Myf5, and c-met, whereas sorted SM/C-2.6-negative cells did not (Supplemental Fig. 3). Thus, the SM/C-2.6 antibody was shown to be useful for isolating living satellite cells by FACS.

We collected all the differentiated ES cells (1×10^6 cells) from cultures on d 3 + 3 + 14. FACS analysis using the SM/C-2.6 antibody showed that 15.7% of the cells were SM/C-2.6 positive (**Fig. 2A**). RT-PCR analysis revealed that sorted SM/C-2.6-positive cells strongly expressed Pax3, Pax7, Myf5, c-met, and M-cadherin (Fig. 2*B*). Using a cytospin preparation of sorted SM/C-2.6-positive cells, we also confirmed the expression of M-cadherin (Fig. 2*C*) and Pax7 (Fig. 2*D*; 70.7±16.5% and 59.9±1.1% positive, respectively); only 2.3 ± 0.49% of the sorted SM/C-2.6-negative cells expressed M-cadherin, and 2.7 ± 0.1% expressed Pax7. Thus, the SM/C-2.6 antibody could enrich for satellite-like cells derived from mES cells *in vitro*.

ES-derived satellite-like cells have strong myogenic potential *in vitro*

To evaluate the myogenic potential of ES-derived SM/C-2.6-positive satellite-like cells *in vitro*, both SM/C-2.6-positive and -negative cells were sorted by FACS and plated in 96-well Matrigel-coated plates (see Fig. 4A). One week after cultivation, the number of muscle fibers in the wells was assessed. Although there were fibroblast-like and endothelium-like cells, MHC-positive fibers (787.3±123.7/well, 10.7±0.8% of the total cells per well, n=3) and Pax7-positive cells (222±81.4/well, 2.9±1.1% of the total cells per well, n=9) were observed in the SM/C-2.6-positive wells. In contrast, very few MHC-positive fibers (8.75±32.6/well, n=15; 0.12±0.46%) or Pax7-positive cells (2.6±2.0/well, n=8; 0.03±0.01%) were seen in the SM/C-2.6-negative wells

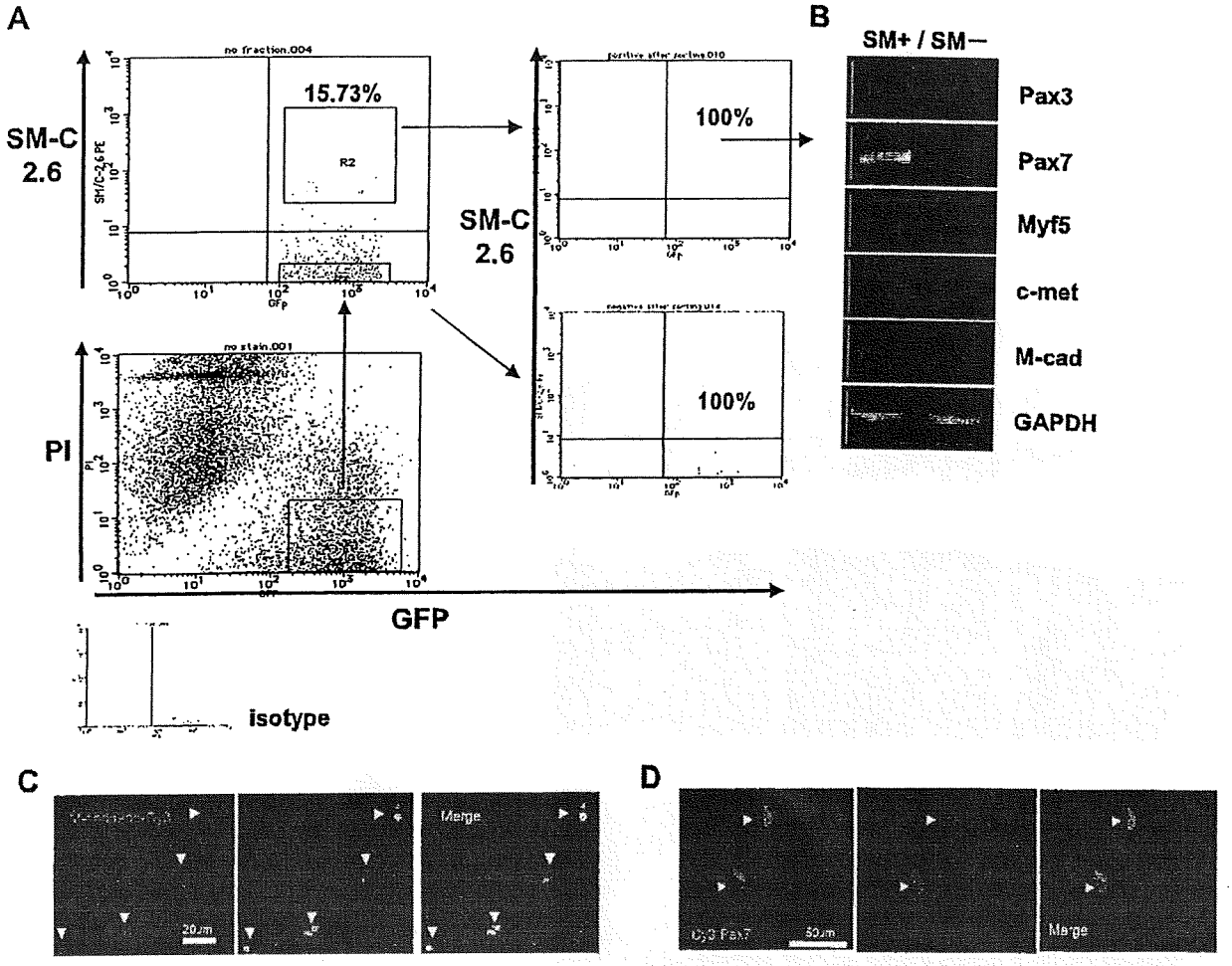

Figure 2. A novel antibody, SM/C-2.6, can enrich Pax7-positive satellite-like cells derived from ES cells. *A*) FACS data of cultured ES cells at d 3 + 3 + 14 indicate that 15.7% of total cultured cells are SM/C-2.6-positive cells. *B*) RT-PCR of the SM/C-2.6-positive fraction showed strong expression of Pax3, Pax7, Myf5, c-met, and M-cadherin. Immunostaining of a cytospin preparation of the sorted SM/C-2.6-positive cells showed that these cells were positive for M-cadherin (*C*), and Pax7 (*D*) (white arrowheads). Scale bars = 20 μm (*C*); 50 μm (*D*).

(both $P<0.05$; **Fig. 3**). Thus, ES-derived satellite-like cells isolated using the SM/C-2.6 antibody possess strong myogenic potential *in vitro*.

Damaged muscle can be repaired by transplantation of ES-derived satellite-like cells

To examine the myogenic potential of ES-derived satellite-like cells *in vivo*, SM/C-2.6-positive and -negative cells were transplanted into conditioned mdx mice (15). The LTA muscles of recipient mdx mice were preinjured with CTX (primary injury; ref. 30) 24 h prior to transplantation, and mice were exposed to 8 cGy of γ-irradiation (whole body) 12 h prior to transplantation (**Fig. 4A**). GFP-positive ES cells were used as donor cells in this experiment. GFP^+ES-derived SM/C-2.6-positive and -negative cells were directly injected into the predamaged LTA muscles. The recipient mice were analyzed 3 wk post-transplantation. By fluorescence stereomicroscopy, GFP-positive tissues were clearly observed within the LTA muscles injected with SM/C-2.6-positive cells (Fig. 4*B* and **Table 1**). In contrast, no GFP-positive tissue was observed in muscles injected with SM/C-2.6-negative cells (Fig. 4*C*). These GFP-positive tissues were further confirmed by diaminobenzidine staining using anti-GFP and a peroxidase-conjugated secondary antibody (Supplemental Fig. 4) to exclude the possibility of autofluorescence of the muscle tissues. Immunostaining with anti-MHC confirmed that these GFP-positive tissues were mature skeletal myofibers (Fig. 4*D*). In addition, GFP/Pax7 double-positive cells were observed within the LTA muscles of the recipient mice (Fig. 4*E* and Supplemental Fig. 5) and in isolated single fibers (Fig. 4*F* and Table 1). The GFP-positive cells were also confirmed to be positive for other satellite cell markers such as Myf5 and M-cadherin (Supplemental Figs. 6 and 7). These GFP/Pax7-double-positive cells were located along the periphery of the muscle fascicle. With laminin immunostaining we verified that the location of the GFP-positive mononuclear cells was between the basal lamina and the muscle cell plasma membrane, a location consistent with the anatomical definition of satellite cells

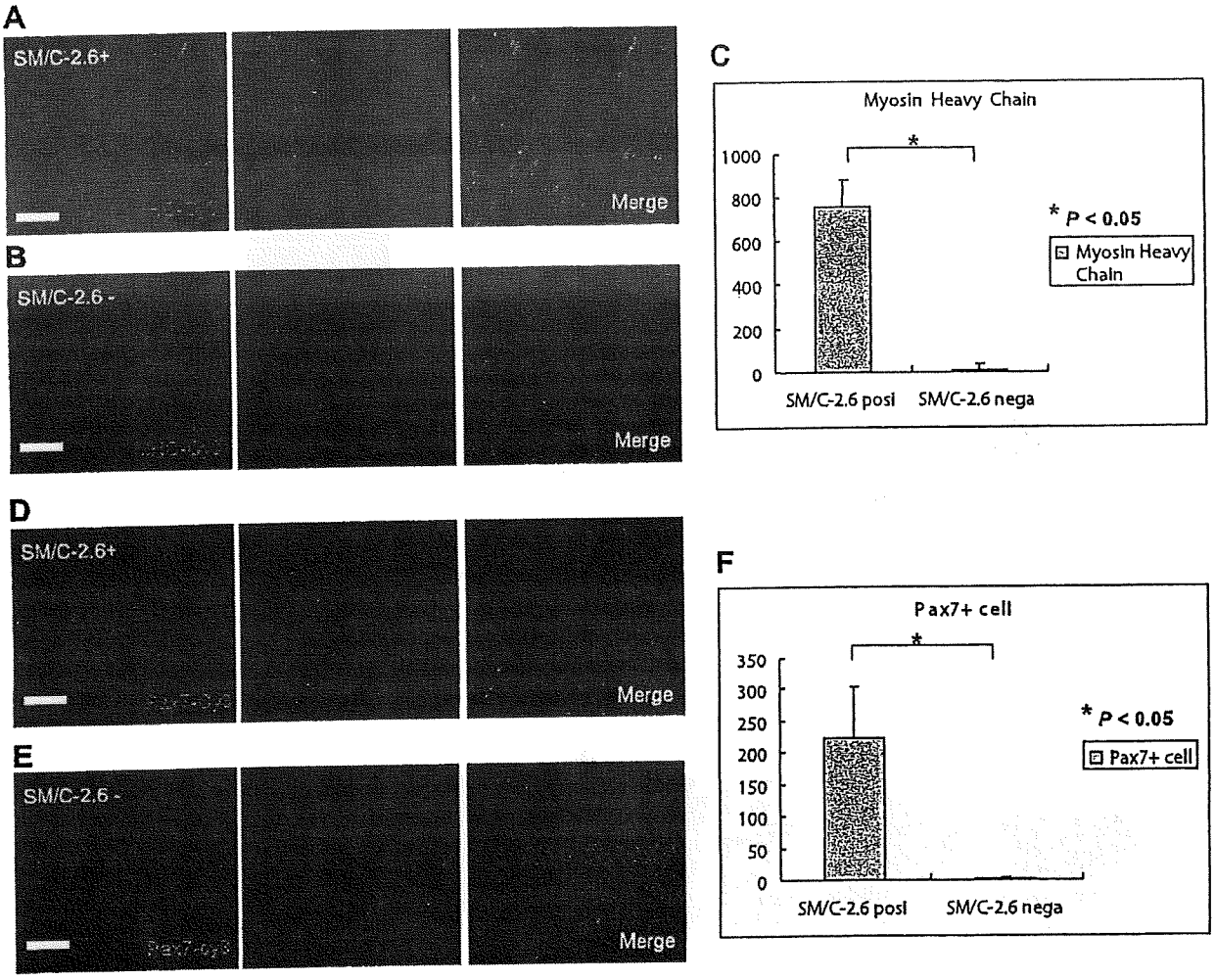

Figure 3. ES-derived satellite-like cells have strong myogenic potential *in vitro*. Immunostaining detected an abundant number of MHC-positive fibers and Pax7-positive cells in SM/C-2.6-positive cell culture (*A*, *D*) but not SM/C-2.6-negative cells (*B*, *E*) after 1 wk in culture. Scale bars = 50 μm. Significant differences were observed in the number of MHC-positive fibers and Pax7-positive cells per well between sorted SM/C-2.6-positive and -negative cell cultures (*C*, *F*).

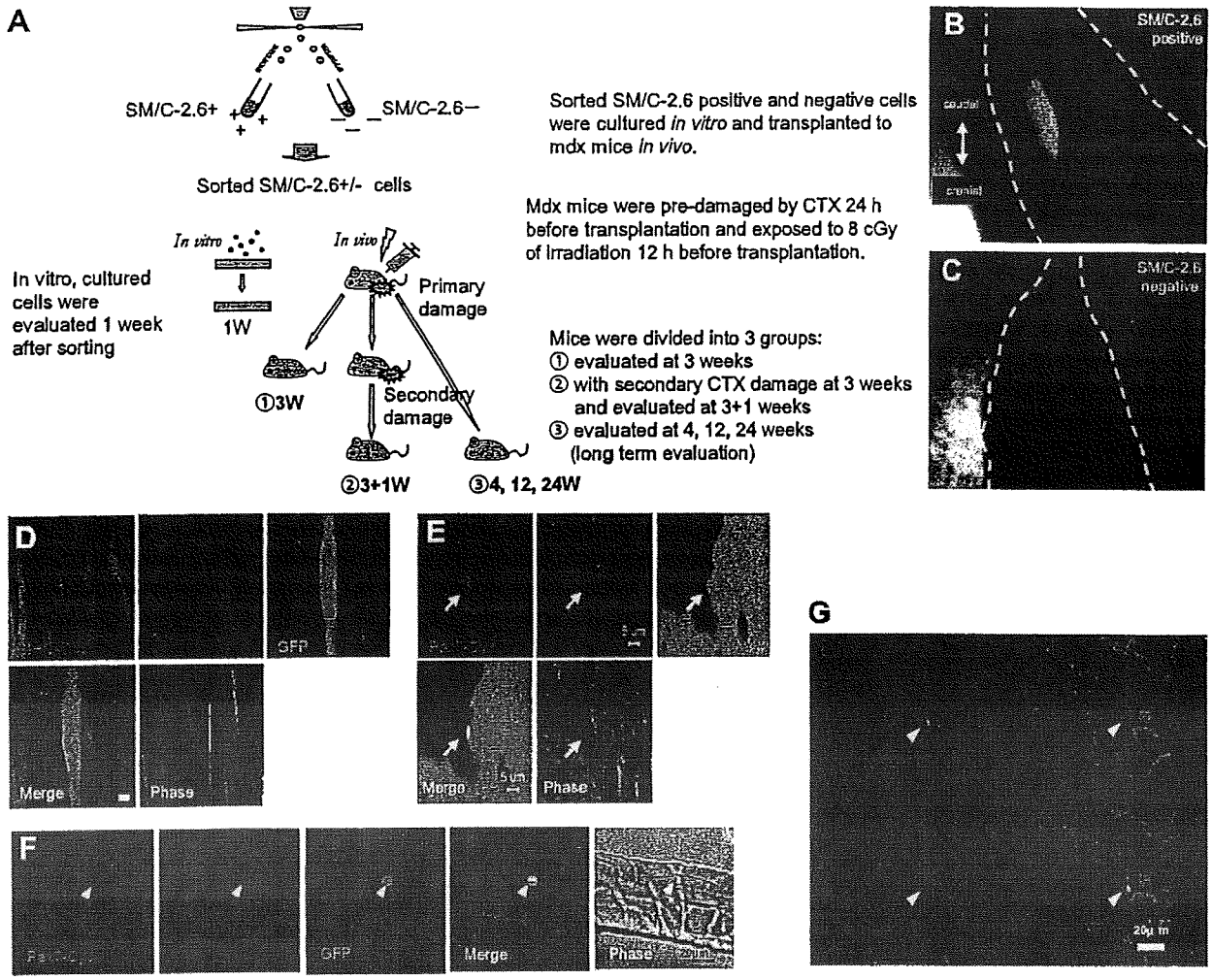

Figure 4. ES-derived satellite-like cells can repair damaged muscle *in vivo*. *A*) Methods for *in vitro* and *in vivo* analysis of sorted SM/C-2.6-positive and -negative cells derived from mES cells. *B, C*) ES-derived GFP-positive tissue engrafted to the LTA muscle of a recipient mouse that received SM/C-2.6-positive cells (*B*) but SM/C-2.6-negative cells (*C*). *D*) Grafted GFP-positive tissues were histologically MHC positive. *E*) GFP/Pax7-double-positive cells were observed in mice that received SM/C-2.6-positive cells by anti-Pax7 immunostaining. *F*) GFP/Pax7-double-positive cells were also confirmed by immunostaining of isolated single fibers. *G*) Laminin immunostaining indicated that the GFP-positive cells were located between the basal lamina and the muscle cell plasma membrane, which is consistent with the anatomical definition of muscle satellite cells. Scale bars = 1 mm (*B, C*); 15 μm (*D*); 5 μm (*E*); 20 μm (*F, G*).

(Fig. 4*G*). In contrast, in mice transplanted with SM/C-2.6-negative cells, GFP-positive tissues were rarely observed, and none of the GFP-positive cells were positive for skeletal MHC. H&E staining indicated that these GFP-positive tissues were surrounded by inflammatory cells (Supplemental Fig. 8), suggesting that these nonmyogenic tissues may undergo phagocytosis. These results demonstrate that ES-derived SM/C-2.6-positive satellite-like cells could be engrafted *in vivo* and repair damaged muscle tissues of the host.

Engrafted ES-derived satellite-like cells function as satellite cells following muscle damage

Muscle satellite cells are generally considered to be self-renewing monopotent stem cells that differentiate into myoblasts and myofibers to repair damaged skeletal muscles. To determine whether these engrafted GFP^+ES-derived satellite-like cells are functional stem cells, we injured the LTA muscle of primary recipient mice 3 wk after primary transplantation with GFP^+SM/C-2.6-positive cells. This experiment let us assess the ability of satellite-like cells to repair damaged muscle fibers and self-renew *in vivo* (14). The LTA muscles were removed and analyzed 1 wk after the secondary injury (reinjured group). Mice that were initially injected with GFP^+SM/C-2.6-positive cells without a second injury were used as a control (nonreinjured group). These control mice were analyzed 3 or 4 wk after transplantation (Fig. 4*A*). GFP-positive muscle fascicles were counted in sections of both reinjured and nonreinjured muscle (Fig. 5*A, B*). In the reinjured group 461.7 ± 117.4 (n=6; per view, ×100) GFP-positive muscle fascicles were observed. In comparison, only 136.7 ± 27.9 (n=4) and 168.7 ± 72.9 (n=6; per view, ×100) GFP-positive muscle fascicles were evident in

TABLE 1. *Transplantation of reinjured and nonreinjured mice and long-term evaluation*

Group	TA with GFP$^+$ fascicles [n(%)][a]	Mouse	Cells/TA injected (n)	GFP$^+$ fascicles/TA (avg)[b]	GFP$^+$/Pax7$^+$ cells/TA (avg)[c]	Engraftment efficiency
SM/C-2.6$^+$						
3W	4/8 (50%)	1	1.75×10^4	125.3	5.3	
		2	3.5×10^4	111.1	7.1	
		3	5×10^4	134.2	5.1	
		4	8×10^4	176.1	4.2	
Mean			$4.5 \pm 2.6 \times 10^4$	136.7 ± 27.0	5.4 ± 1.2	0.30%
4W	6/9 (66.67%)	1	2×10^4	77.3	6.1	
		2	1.3×10^5	153.2	4.6	
		3	5×10^4	163.1	6.8	
		4	3.5×10^4	168.9	5.1	
		5	8×10^4	281.1	7.2	
		6	1.75×10^4	169.4	6.2	
Mean			$3.6 \pm 2.5 \times 10^4$	168.7 ± 72.9	6 ± 1	0.47%
3 + 1W	6/8 (75%)	1	2×10^4	581.2	11.2	
		2	1.3×10^5	370.3	11.5	
		3	5×10^4	586.6	10.1	
		4	3.5×10^4	486.6	5.9	
		5	8×10^4	347.1	15.3	
		6	1.75×10^4	542.9	10.8	
Mean			$5.5 \pm 4.3 \times 10^4$	461.7 ± 117.3	10.8 ± 3	0.84%
12W	3/5 (60%)	1	2×10^4	391.5	9.7	
		2	5×10^4	266	9.3	
		3	8×10^4	280.2	6	
Mean			$5 \pm 3 \times 10^4$	312.6 ± 68.7	8.3 ± 2	0.59%
24W	1/2 (50%)	1	2×10^4	58.62	3.45	
Mean			2×10^4	58.62	3.45	0.20%
SM/C-2.6$^-$						
3W	0/8 (0%)	1–8	$1–8 \times 10^4$	0	0	0%
4W	0/9 (0%)	1–9	$1.3–8 \times 10^4$	0	0	0%
3 + 1W	0/8 (0%)	1–8	$1.75–13 \times 10^4$	0	0	0%
12W	0/5 (0%)	1–8	$2–8 \times 10^4$	0	0	0%
24W	0/2 (0%)	1–2	2×10^4	0	0	0%

Serial transplantation

	Primary transplantation		Secondary transplantation		
Mouse	Cells injected	Collected GFP$^+$ cells/TA	Cells injected	GFP$^+$ fascicles/TA	Engraftment efficiency
1	2×10^4	3253	200	29.3	14.7%
2	2×10^4	2277	200	28.6	14.3%
Mean	2×10^4	2765	200	29 ± 0.5	14.5%

TA, tibialis anterior; 3W, nonreinjured group analyzed 3 wk after cell transplantation; 4W, nonreinjured group analyzed 4 wk after cell transplantation; 3 + 1W, reinjured group reinjured 3 wk after cell transplantation and analyzed 1 wk after reinjury; 12W, long-term engraftment evaluation analyzed 12 wk after cell transplantation; 24W, long-term engraftment evaluation analyzed 24 wk after cell transplantation. [a]Percentage of TA that had engrafted with GFP$^+$ fibers was calculated as number of TAs with GFP$^+$ fibers/total TAs injected with cells. [b]Average determined from number of GFP$^+$ muscle fascicles counted per field at ×100 in 10 fields. [c]Average determined from number of GFP$^+$/Pax7+ cells counted per field at ×100 in 10 fields.

the nonreinjured groups at 3 and 4 wk, respectively, after transplantation (Fig. 5*B* and Table 1). Furthermore, we also observed that many GFP-positive muscle fibers had a typical central nucleus in the reinjured group (Fig. 5*C*), indicating regenerating muscle fibers. Taken together, these results suggest that these GFP-positive muscle tubes were freshly regenerated by the engrafted GFP$^+$ ES-derived satellite-like cells in response to the second injury. Surprisingly, immunostaining with anti-Pax7 revealed an increase in number of GFP/Pax7-double-positive cells in the reinjured group (10.8±3.0/view compared to 5.4±1.2, and 6.0±1.0 in the nonreinjured group; Fig. 5*D* and Table 1). This result strongly suggests that engrafted ES-derived satellite-like cells not only self-renewed but also expanded in number, possibly replacing the recipient satellite cells lost because of excessive repair of skeletal muscle in response to the second injury.

ES-derived satellite-like cells are capable of long-term engraftment in recipient muscles

Long-term engraftment is an important characteristic of self-renewing stem cells. If these ES-derived satellite-

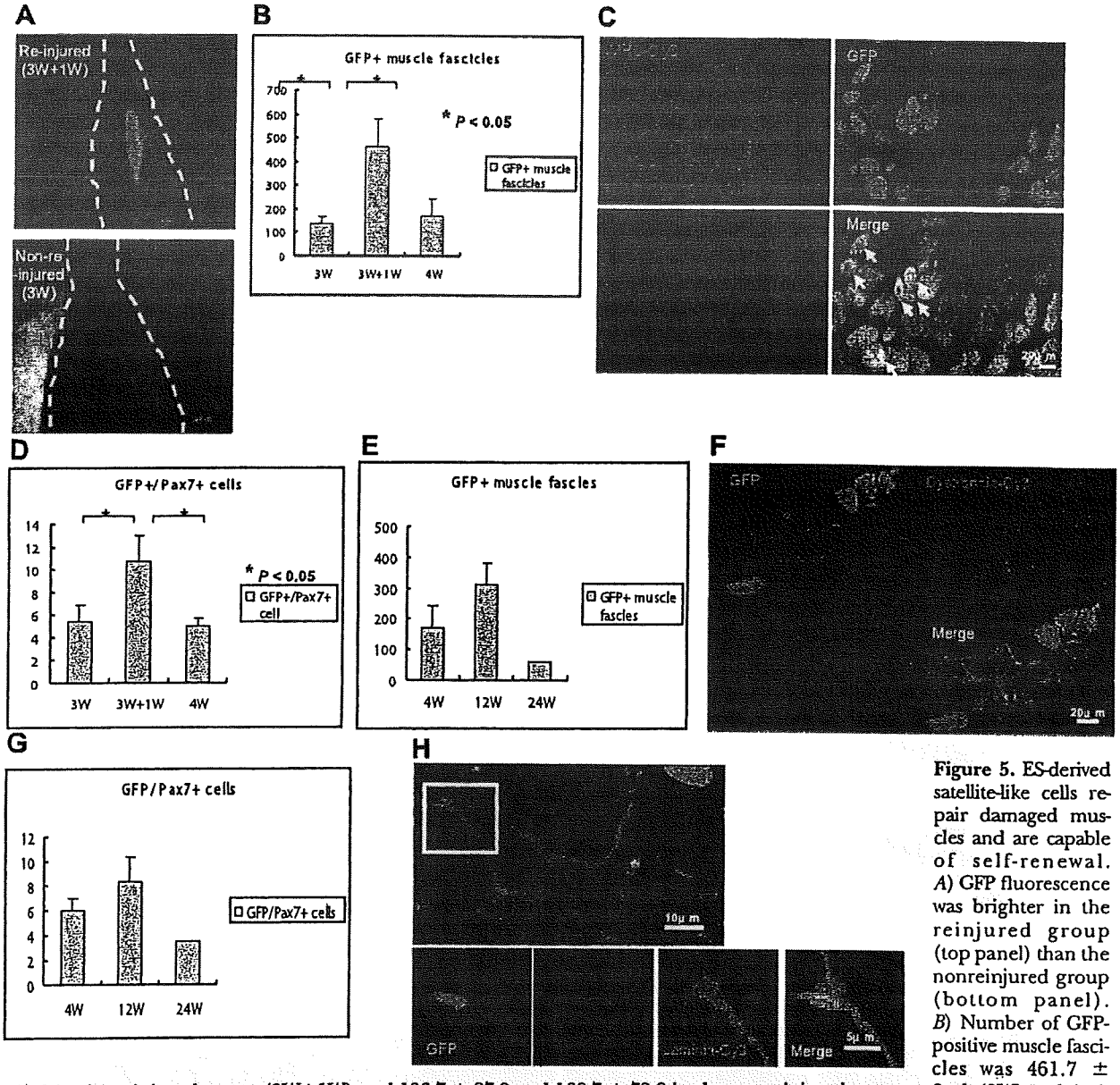

Figure 5. ES-derived satellite-like cells repair damaged muscles and are capable of self-renewal. *A*) GFP fluorescence was brighter in the reinjured group (top panel) than the nonreinjured group (bottom panel). *B*) Number of GFP-positive muscle fascicles was 461.7 ± 117.3 in the reinjured group (3W+1W) and 136.7 ± 27.9 and 168.7 ± 72.9 in the nonreinjured group at 3 wk (3W) and 4 wk (4W), respectively. *C*) GFP-positive fibers were confirmed to be MHC positive and contained central nuclei (arrows). *D*) Number of GFP/Pax7-double-positive cells also increased significantly in the reinjured group (10.8±3.0 cells at 3W+1W) compared to the nonreinjured group (5.4±1.2 and 6.0±1.0 at 3W and 4W, respectively). *E*) In long-term evaluations, number of GFP-positive muscle fascicles at 12 wk (12W) increased relative to number at 4 wk after transplantation [312.6±68.7 (n=3) *vs.* 168.7±72.9]. However, a decrease was observed at 24 wk (58.6; n=1). *F*) Immunostaining showed dystrophin (red) surrounding the donor-derived GFP-positive fibers (green), 24 wk after transplantation of SM/C-2.6-positive cells. *G*) Results similar to *E* were observed with the number of GFP/Pax7-double-positive cells. *H*) A GFP-positive cell beneath the basal lamina was observed. Scale bars = 1 mm (*A*); 20 μm (*C*); 20 μm (*F*); 10 μm (*H*, top panel); 5 μm (*H*, bottom panels).

like cells function as normal stem cells in skeletal muscle, they should be able to reside within the tissue for long periods of time and undergo asymmetric cell divisions to maintain the number of satellite cells and to generate muscle fibers. To examine this stem cell function, we analyzed the recipient mice at 4, 12, and 24 wk after transplantation. Intriguingly, in the LTA muscle of mdx mice transplanted with SM/C-2.6-positive cells, the number of GFP-positive fascicles at 12 wk increased over that at 4 wk [12.6±68.7 (n=3) *vs.* 168.7±72.9; Fig. 5*E*] but decreased by 24 wk (58.6; n=1). These engrafted GFP-positive tissues were confirmed to be MHC positive through immunostaining (Supplemental Fig. 9), and surrounding these GFP-positive fibers, dystrophin was observed (Fig. 5*F*). The numbers of GFP/Pax7-double-positive cells were maintained from week 4 to week 24 (Fig. 5*G*, Table 1, and Supplemental Fig. 10) and the location of GFP-positive cells under the basal lamina meets the anatomical definition of satellite cells (Fig. 5*H*). No teratomas were

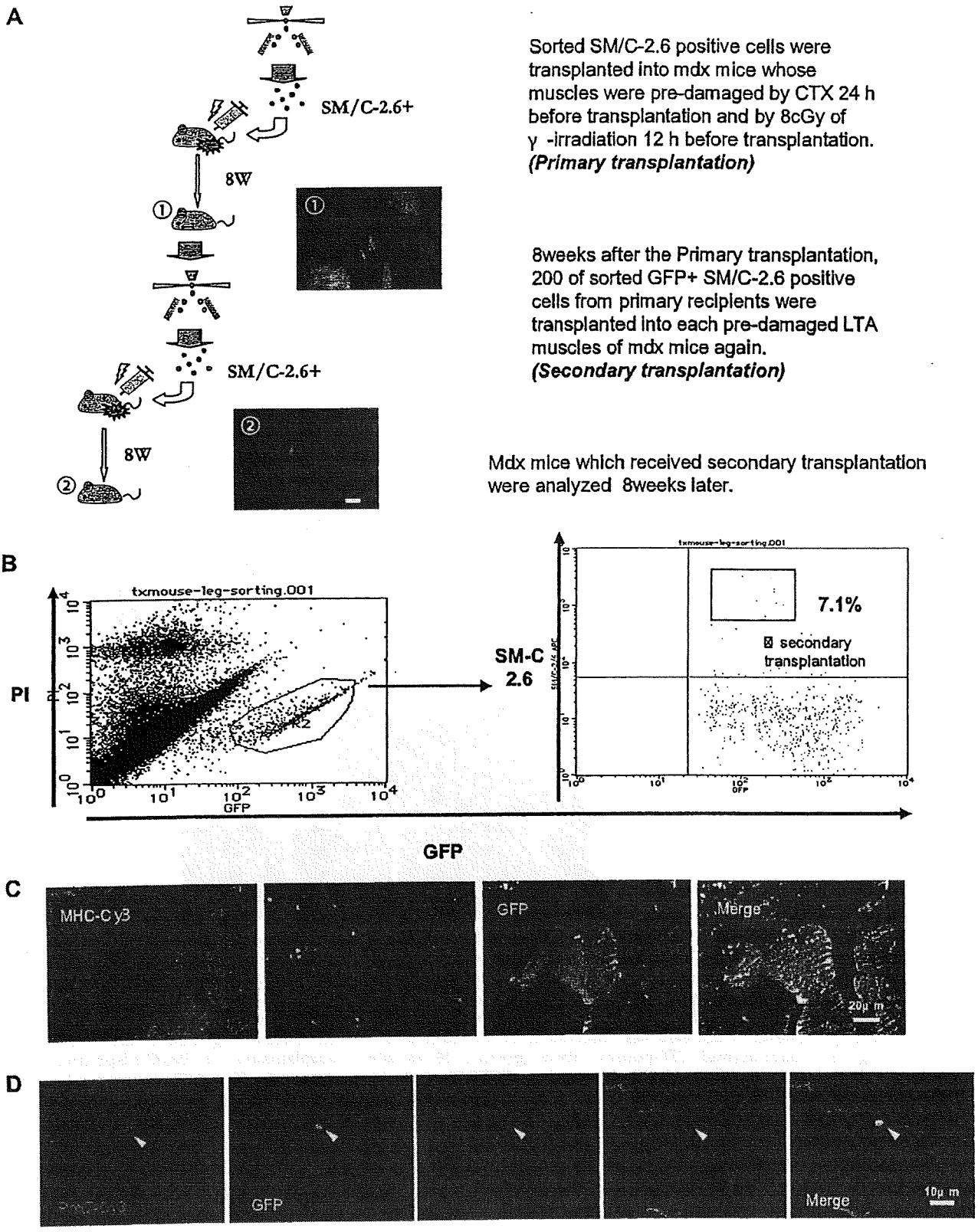

Figure 6. ES-derived satellite-like cells can be secondarily transplanted. *A*) SM/C-2.6-positive cells (2.5×10^4) were transplanted into the LTA muscle of recipient mice in primary transplantation, and as few as 200 SM/C-2.6-positive cells collected from the primary recipients were retransplanted (secondary transplantation) into the LTA muscle of secondary recipient mice. *B*) FACS data of primary transplantation indicated that 7.1% of engrafted (GFP-positive) cells were SM/C-2.6-positive. *C*) Eight weeks after secondary transplantation, immunostaining of LTA muscle for MHC showed that engrafted ES-derived GFP-positive tissues formed mature skeletal muscle fibers. *D*) GFP/Pax7-double-positive cells (arrowhead) located beneath the basal lamina were observed within GFP-positive LTA muscle of secondary recipient mice. Scale bars = 2 mm (*A*); 20 μm (*C*); 10 μm (*D*).

found in recipient mice transplanted with SM/C-2.6-positive cells. Thus, ES-derived satellite-like cells effectively engrafted and provided long-term stem cells, which played an important role in maintenance of the integrity of the surrounding muscle tissue.

ES-derived satellite-like cells can be secondarily transplanted

For a more thorough characterization of the ES-derived satellite-like cells, we performed serial transplantations. Eight weeks after the primary cell transplantation with 2×10^4 SM/C-2.6-positive cells, the LTA muscles of the primary recipient mice were dissected to isolate the engrafted ES-derived cells, 2765 ± 685.9 (n=2; **Fig. 6*A***). The GFP^+/SM/C-2.6-positive cells within the engrafted cells were sorted by FACS (204±33.9; n=2), and only 200 GFP+/SM/C-2.6-positive cells/mouse were transplanted into predamaged LTA muscles of mdx mice (Fig. 6*B*). Eight weeks later (16 wk after the primary transplantation), the recipient mice were analyzed. GFP-positive tissue in the LTA muscle of the secondary recipient mice was observed (Fig. 6*A*). The GFP-positive tissues were confirmed to be MHC-positive mature skeletal muscle (Fig. 6*C*), and surrounding these engrafted GFP-positive skeletal muscle fascicles, dystrophin was observed (Supplemental Fig. 11). GFP/Pax7-double-positive cells located beneath the basal lamina were also detected in the engrafted tissue (Fig. 6*D*). Thus, with only 200 GFP^+SMC/2.6-positive cells, injured skeletal muscle and Pax7+ cells were successfully restored in the secondary recipients. These findings demonstrate that stem cell fraction contained within SM/C-2.6-positive cells was enriched *in vivo* through transplantation.

DISCUSSION

Many attempts have been made to induce mES cells into the skeletal muscle lineage, with hanging drop cultures for EB formation being the most widely applied method (25). However, although EBs contain cells derived from all 3 germ layers, effective induction of mES cells into the myogenic lineage, including myogenic stem cells (satellite cells), has not yet been achieved. Because of the lack of adequate surface markers, purifying ES-derived myogenic precursor/stem cells from differentiated mES cells *in vitro* has been difficult. To overcome these problems, we modified the classic EB culture system by combining it with aspects of the single-fiber culture method. Single-fiber culture (33) has been used for functional evaluation of satellite cells. When a single myofiber is plated on a Matrigel-coated plate with DMEM containing HS, satellite cells migrate out of the fiber and differentiate into myoblasts to form myofibers *in vitro*. Matrigel allows the migrating satellite cells to proliferate before differentiating and fusing into large multinucleated myotubes (35). We hypothesized that this Matrigel environment might be suitable for ES cell differentiation into satellite cells and myoblasts. Therefore, we introduced Matrigel and HS into the classic EB culture system and established an efficient induction system for myogenic lineage cells, including cells expressing Pax7, a commonly recognized marker for skeletal muscle stem cells. Furthermore, we also successfully enriched ES-derived Pax7-positive myogenic precursor/stem cells using the SM/C-2.6 antibody.

The steps in ES cell induction are thought to be homologous to normal embryogenesis. During normal skeletal myogenesis, the initial wave of myogenic precursor cells in the dermomyotome express Myf5/MRF4 and Pax3, followed by a wave of Pax3/Pax7 expression (36). These waves of myogenesis act upstream of the primary myogenic transcription factor MyoD (37-39). In myotome formation skeletal myogenesis begins with myoblasts, termed somitic myoblasts, which appear at approximately E8.5, followed by the appearance of embryonic myoblasts (E11.5), fetal myoblasts (E16.5), and, ultimately, satellite cells, which are responsible for postnatal muscle regeneration (40). Our RT-PCR results (Fig. 1*J*) showed an earlier appearance of Pax3 expression, on d 3 + 3, followed by Pax3/Pax7 expression on d 3 + 3 + 7 and stronger expression of Pax3 than Pax7. These results resemble normal myogenesis, in which the primary wave of myogenesis is followed by a secondary wave of Pax3/Pax7-dependent myogenesis (41). Considering that in the time course of myogenesis satellite cells emerge during late fetal development, ES-derived Pax7-positive cells were collected on d 3 + 3 + 14 in an attempt to acquire cells that correspond to those of the late fetal to neonatal period. However, RT-PCR results of myogenic factors in SM/C-2.6-positive cells (Fig. 2*B*) indicated that these ES-derived SM/C-2.6-positive cells are a heterogeneous population, because they express not only Pax3 and Pax7 but also Myf5 and c-met. Although further confirmation is needed, we hypothesize that both embryonic/fetal myoblasts expressing Myf-5 and/or c-met and satellite/long-term stem cells expressing Pax3/Pax7 are present.

To confirm that the ES-derived SM/C-2.6-positive cell population contained functional satellite cells, the muscle regeneration and self-renewal capacities were examined. Recently Collins *et al.* established an excellent system in which sequential damage to the muscle of a recipient mouse was applied, to evaluate both muscle regeneration and self-renewal (14) Using their experimental approach, a significant increase in numbers of both ES-derived GFP-positive muscle fascicles and GFP/Pax7-double-positive cells was observed in mice that received a second injury. This result not only demonstrates the myogenic ability of ES-derived cells but also strongly supports the idea that these cells undergo self-renewal *in vivo*.

Analysis of long-term engraftment is an important method to verify self-renewal ability, for 2 reasons. First, ES-derived satellite cells must be able to engraft for long periods of time in order to provide the amount of progeny needed for repairing damaged tissue for an

extended period. In our study the ES-derived GFP-positive skeletal muscle tissues and Pax7-positive cells engrafted up to 24 wk and were located beneath the basal lamina, which is consistent with the anatomical definition of satellite cells. Although the number of GFP-positive fascicles at 24 wk decreased compared to 12 wk, this diminution may be due to the heterogeneity of ES-derived SM/C-2.6-positive cells as we mentioned. Because myoblasts cannot support myogenesis in the long term, we believe that GFP-positive fascicles at 24 wk are products of ES-derived satellite-like cells. Second, one of the potential risks of ES cell transplantation is teratoma formation. Considering clinical applications, it is extremely important to prevent formation of teratomas in the recipients. In our study more than 60 transplanted mice were evaluated through gross morphological and histological examination. There were no teratomas formed in mice that received SM/C-2.6-positive cells, and only 1 teratoma was found among the mice that received SM/C-2.6-negative cells. This result suggests that the risk of tumor formation by the ES cells was eliminated by using sorted SM/C-2.6-positive cells.

In addition to the sequential damage model and the long-term engraftment evaluation, we performed serial transplantations to further confirm the stem cell properties of these ES-derived SM/C-2.6-positive cells. Serial transplantation enables the identification and separation of long-term stem cells from short-term progenitors (42). To eliminate myoblast involvement, we designed a serial transplantation protocol of 8 + 8 wk (*i.e.*, a second transplantation 8 wk after the primary transplantation and an analysis of recipient mice 8 wk after the second transplantation). Strikingly these recollected ES-derived SM/C-2.6-positive cells showed significantly higher engraftment efficiency compared to the primary transplantation. In the previous reports engraftment efficiencies of myoblasts transplantation was ~0.1-0.2%, with the highest reported value being 2% (43-45). This engraftment efficiency is similar to our primary transplantation (0.2-0.8%) as well as the plating efficiency of SM/C-2.6-positive cells *in vitro* (0.07%). In our study as few as 200 recollected ES-derived SM/C-2.6-positive cells were transplanted in the second transplantation, and 29.0 ± 0.47 (n=2) fascicles were observed, which indicates 14.7% of higher engraftment efficiency. Thus, through the serial transplantation, ES-derived stem cell fraction was purified. A comparison of these SM/C-2.6-positive cells before and after injection might help to characterize the stem cell fraction derived from ES cells.

There have been few reports describing transplantation of ES-derived myogenic cells into injured muscles, and the report of engraftable skeletal myoblasts derived from human ES cells represents significant progress (26). Recently Darabi *et al.* (46) have reported that by introducing Pax3 into mouse embryoid bodies, autonomous myogenesis was initiated *in vitro*, and Pax3-induced cells regenerated skeletal muscles *in vivo* by sorting the PDGF-a+Flk-1- cells. The Pax3 expression was not observed until 7 d of differentiation culture, but introduced Pax3 expression pushed EBs to myogenic differentiation. Interestingly, we observed Pax3 expression at d 3 + 3 weakly and d 3 + 3 + 7 strongly, and gene expression process in our culture is very similar to theirs. In prolonged culture using Matrigel and HS, EBs were able to initiate myogenesis without gene modification in our system.

In conclusion, we successfully generated transplantable myogenic cells, including satellite-like cells, from mES cells. The ES-derived myogenic precursor/stem cells could be enriched using a novel antibody, SM/C-2.6. These ES-derived SM/C-2.6-positive cells possess a high myogenic potential, participate in muscle regeneration, and are located beneath the basal lamina where satellite cells normally reside. The self-renewal of these ES-derived satellite-like cells enabled them to survive long-term engraftment, up to 24 wk. Through serial transplantation, these ES-derived SM/C-2.6-positive cells were further enriched and produced a high engraftment efficiency of 14.7%.

Our success in inducing mES cells to form functional muscle stem cells, the satellite-like cells, will provide an important foundation for clinical applications in the treatment of DMD patients. Fj

This work was supported by a Grant-in-Aid for Scientific Research (S) (19109006) and a Grant-in-Aid for Scientific Research (B) (18390298) from the Ministry of Education, Science, Technology, Sports, and Culture of Japan.

REFERENCES

1. Nawrotzki, R., Blake, D. J., and Davies, K. E. (1996) The genetic basis of neuromuscular disorders. *Trends Genet.* **12**, 294–298
2. Emery, A. E. (2002) The muscular dystrophies. *Lancet* **359**, 687–695
3. Michalak, M., and Opas, M. (1997) Functions of dystrophin and dystrophin associated proteins. *Curr. Opin. Neurol.* **10**, 436–442
4. Suzuki, A., Yoshida, M., Hayashi, K., Mizuno, Y., Hagiwara, Y., and Ozawa, E. (1994) Molecular organization at the glycoprotein-complex-binding site of dystrophin. Three dystrophin-associated proteins bind directly to the carboxy-terminal portion of dystrophin. *Eur. J. Biochem./FEBS* **220**, 283–292
5. Bonilla, E., Samitt, C. E., Miranda, A. F., Hays, A. P., Salviati, G., DiMauro, S., Kunkel, L. M., Hoffman, E. P., and Rowland, L. P. (1988) Duchenne muscular dystrophy: deficiency of dystrophin at the muscle cell surface. *Cell* **54**, 447–452
6. Mauro, A. (1961) Satellite cell of skeletal muscle fibers. *J. Biophys. Biochem. Cytol.* **9**, 493–495
7. Moss, F. P., and Leblond, C. P. (1971) Satellite cells as the source of nuclei in muscles of growing rats. *Anat. Rec.* **170**, 421–435
8. Snow, M. H. (1978) An autoradiographic study of satellite cell differentiation into regenerating myotubes following transplantation of muscles in young rats. *Cell Tissue Res.* **186**, 535–540
9. Jejurikar, S. S., and Kuzon, W. M., Jr. (2003) Satellite cell depletion in degenerative skeletal muscle. *Apoptosis* **8**, 573–578
10. Schultz, E., and Jaryszak, D. L. (1985) Effects of skeletal muscle regeneration on the proliferation potential of satellite cells. *Mech. Ageing Dev.* **30**, 63–72
11. Webster, C., and Blau, H. M. (1990) Accelerated age-related decline in replicative life-span of Duchenne muscular dystrophy myoblasts: implications for cell and gene therapy. *Somat. Cell Mol. Genet.* **16**, 557–565
12. Hashimoto, N., Murase, T., Kondo, S., Okuda, A., and Inagawa-Ogashiwa, M. (2004) Muscle reconstitution by muscle satellite

cell descendants with stem cell-like properties. *Development (Camb.)* **131**, 5481–5490
13. Montarras, D., Morgan, J., Collins, C., Relaix, F., Zaffran, S., Cumano, A., Partridge, T., and Buckingham, M. (2005) Direct isolation of satellite cells for skeletal muscle regeneration. *Science* **309**, 2064–2067
14. Collins, C. A., Olsen, I., Zammit, P. S., Heslop, L., Petrie, A., Partridge, T. A., and Morgan, J. E. (2005) Stem cell function, self-renewal, and behavioral heterogeneity of cells from the adult muscle satellite cell niche. *Cell* **122**, 289–301
15. Partridge, T. A., Morgan, J. E., Coulton, G. R., Hoffman, E. P., and Kunkel, L. M. (1989) Conversion of mdx myofibres from dystrophin-negative to -positive by injection of normal myoblasts. *Nature* **337**, 176–179
16. Mendell, J. R., Kissel, J. T., Amato, A. A., King, W., Signore, L., Prior, T. W., Sahenk, Z., Benson, S., McAndrew, P. E., Rice, R., Nagaraja, H., Stephens, R., Lantry, L., Morris, G. E., and Burghes, A. H. M. (1995) Myoblast transfer in the treatment of Duchenne's muscular dystrophy. *N. Engl. J. Med.* **333**, 832–838
17. Weissman, I. L., Anderson, D. J., and Gage, F. (2001) Stem and progenitor cells: origins, phenotypes, lineage commitments, and transdifferentiations. *Annu. Rev. Cell Dev. Biol.* **17**, 387–403
18. Relaix, F., Montarras, D., Zaffran, S., Gayraud-Morel, B., Rocancourt, D., Tajbakhsh, S., Mansouri, A., Cumano, A., and Buckingham, M. (2006) Pax3 and Pax7 have distinct and overlapping functions in adult muscle progenitor cells. *J. Cell Biol.* **172**, 91–102
19. Seale, P., Sabourin, L. A., Girgis-Gabardo, A., Mansouri, A., Gruss, P., and Rudnicki, M. A. (2000) Pax7 is required for the specification of myogenic satellite cells. *Cell* **102**, 777–786
20. Cornelison, D. D., and Wold, B. J. (1997) Single-cell analysis of regulatory gene expression in quiescent and activated mouse skeletal muscle satellite cells. *Dev. Biol.* **191**, 270–283
21. Hollnagel, A., Grund, C., Franke, W. W., and Arnold, H. H. (2002) The cell adhesion molecule M-cadherin is not essential for muscle development and regeneration. *Mol. Cell. Biol.* **22**, 4760–4770
22. Bottaro, D. P., Rubin, J. S., Faletto, D. L., Chan, A. M., Kmiecik, T. E., Vande Woude, G. F., and Aaronson, S. A. (1991) Identification of the hepatocyte growth factor receptor as the c-met proto-oncogene product. *Science* **251**, 802–804
23. Fukada, S., Higuchi, S., Segawa, M., Koda, K., Yamamoto, Y., Tsujikawa, K., Kohama, Y., Uezumi, A., Imamura, M., Miyagoe-Suzuki, Y., Takeda, S., and Yamamoto, H. (2004) Purification and cell-surface marker characterization of quiescent satellite cells from murine skeletal muscle by a novel monoclonal antibody. *Exp. Cell Res.* **296**, 245–255
24. Dekel, I., Magal, Y., Pearson-White, S., Emerson, C. P., and Shani, M. (1992) Conditional conversion of ES cells to skeletal muscle by an exogenous MyoD1 gene. *New Biol.* **4**, 217–224
25. Rohwedel, J., Maltsev, V., Bober, E., Arnold, H. H., Hescheler, J., and Wobus, A. M. (1994) Muscle cell differentiation of embryonic stem cells reflects myogenesis in vivo: developmentally regulated expression of myogenic determination genes and functional expression of ionic currents. *Dev. Biol.* **164**, 87–101
26. Barberi, T., Bradbury, M., Dincer, Z., Panagiotakos, G., Socci, N. D., and Studer, L. (2007) Derivation of engraftable skeletal myoblasts from human embryonic stem cells. *Nat. Med.* **13**, 642–648
27. Doetschman, T. C., Eistetter, H., Katz, M., Schmidt, W., and Kemler, R. (1985) The in vitro development of blastocyst-derived embryonic stem cell lines: formation of visceral yolk sac, blood islands and myocardium. *J. Embryol. Exp. Morphol.* **87**, 27–45
28. Niwa, H., Yamamura, K., and Miyazaki, J. (1991) Efficient selection for high-expression transfectants with a novel eukaryotic vector. *Gene* **108**, 193–199
29. Yoshimoto, M., Chang, H., Shiota, M., Kobayashi, H., Umeda, K., Kawakami, A., Heike, T., and Nakahata, T. (2005) Two different roles of purified CD45+c-Kit+Sca-1+Lin-cells after transplantation in muscles. *Stem Cells (Dayton)* **23**, 610–618
30. Harris, J. B. (2003) Myotoxic phospholipases A2 and the regeneration of skeletal muscles. *Toxicon* **42**, 933–945
31. Fukada, S., Miyagoe-Suzuki, Y., Tsukihara, H., Yuasa, K., Higuchi, S., Ono, S., Tsujikawa, K., Takeda, S., and Yamamoto, H. (2002) Muscle regeneration by reconstitution with bone marrow or fetal liver cells from green fluorescent protein-gene transgenic mice. *J. Cell Sci.* **115**, 1285–1293
32. Gross, J. G., and Morgan, J. E. (1999) Muscle precursor cells injected into irradiated mdx mouse muscle persist after serial injury. *Muscle Nerve* **22**, 174–185
33. Rosenblatt, J. D., Lunt, A. I., Parry, D. J., and Partridge, T. A. (1995) Culturing satellite cells from living single muscle fiber explants. *In Vitro Cell. Dev. Biol.* **31**, 773–779
34. Dhawan, J., and Rando, T. A. (2005) Stem cells in postnatal myogenesis: molecular mechanisms of satellite cell quiescence, activation and replenishment. *Trends Cell Biol.* **15**, 666–673
35. Zammit, P. S., Relaix, F., Nagata, Y., Ruiz, A. P., Collins, C. A., Partridge, T. A., and Beauchamp, J. R. (2006) Pax7 and myogenic progression in skeletal muscle satellite cells. *J. Cell Sci.* **119**, 1824–1832
36. Relaix, F., Rocancourt, D., Mansouri, A., and Buckingham, M. (2005) A Pax3/Pax7-dependent population of skeletal muscle progenitor cells. *Nature* **435**, 948–953
37. Tajbakhsh, S., Rocancourt, D., Cossu, G., and Buckingham, M. (1997) Redefining the genetic hierarchies controlling skeletal myogenesis: Pax-3 and Myf-5 act upstream of MyoD. *Cell* **89**, 127–138
38. Kiefer, J. C., and Hauschka, S. D. (2001) Myf-5 is transiently expressed in nonmuscle mesoderm and exhibits dynamic regional changes within the presegmented mesoderm and somites I-IV. *Dev. Biol.* **232**, 77–90
39. Hirsinger, E., Malapert, P., Dubrulle, J., Delfini, M. C., Duprez, D., Henrique, D., Ish-Horowicz, D., and Pourquie, O. (2001) Notch signalling acts in postmitotic avian myogenic cells to control MyoD activation. *Development (Camb.)* **128**, 107–116
40. Smith, T. H., Block, N. E., Rhodes, S. J., Konieczny, S. F., and Miller, J. B. (1993) A unique pattern of expression of the four muscle regulatory factor proteins distinguishes somitic from embryonic, fetal and newborn mouse myogenic cells. *Development (Camb.)* **117**, 1125–1133
41. Kassar-Duchossoy, L., Giacone, E., Gayraud-Morel, B., Jory, A., Gomes, D., and Tajbakhsh, S. (2005) Pax3/Pax7 mark a novel population of primitive myogenic cells during development. *Genes Dev.* **19**, 1426–1431
42. Harrison, D. E., Astle, C. M., and Delaittre, J. A. (1978) Loss of proliferative capacity in immunohemopoietic stem cells caused by serial transplantation rather than aging. *J. Exp. Med.* **147**, 1526–1531
43. Yao, S. N., and Kurachi, K. (1993) Implanted myoblasts not only fuse with myofibers but also survive as muscle precursor cells. *J. Cell Sci.* **105**(Pt. 4), 957–963
44. Rando, T. A., and Blau, H. M. (1994) Primary mouse myoblast purification, characterization, and transplantation for cell-mediated gene therapy. *J. Cell Biol.* **125**, 1275–1287
45. Sherwood, R. I., Christensen, J. L., Conboy, I. M., Conboy, M. J., Rando, T. A., Weissman, I. L., and Wagers, A. J. (2004) Isolation of adult mouse myogenic progenitors: functional heterogeneity of cells within and engrafting skeletal muscle. *Cell* **119**, 543–554
46. Darabi, R., Gehlbach, K., Bachoo, R. M., Kamath, S., Osawa, M., Kamm, K. E., Kyba, M., and Perlingeiro, R. C. (2008) Functional skeletal muscle regeneration from differentiating embryonic stem cells. *Nat. Med.* **14**, 134–143

Received for publication October 21, 2008.
Accepted for publication January 8, 2009.

Efficacy of Systemic Morpholino Exon-Skipping in Duchenne Dystrophy Dogs

Toshifumi Yokota, PhD,[1] Qi-long Lu, MD, PhD,[2] Terence Partridge, PhD,[1] Masanori Kobayashi, DVM,[3] Akinori Nakamura, MD, PhD,[3] Shin'ichi Takeda, MD, PhD,[3] and Eric Hoffman, PhD[1]

Objective: Duchenne muscular dystrophy (DMD) is caused by the inability to produce dystrophin protein at the myofiber membrane. A method to rescue dystrophin production by antisense oligonucleotides, termed *exon-skipping,* has been reported for the *mdx* mouse and in four DMD patients by local intramuscular injection. We sought to test efficacy and toxicity of intravenous oligonucleotide (morpholino)-induced exon skipping in the DMD dog model.

Methods: We tested a series of antisense drugs singly and as cocktails, both in primary cell culture, and two *in vivo* delivery methods (intramuscular injection and systemic intravenous injection). The efficiency and efficacy of multiexon skipping (exons 6–9) were tested at the messenger RNA, protein, histological, and clinical levels.

Results: Weekly or biweekly systemic intravenous injections with a three-morpholino cocktail over the course of 5 to 22 weeks induced therapeutic levels of dystrophin expression throughout the body, with an average of about 26% normal levels. This was accompanied by reduced inflammatory signals examined by magnetic resonance imaging and histology, improved or stabilized timed running tests, and clinical symptoms. Blood tests indicated no evidence of toxicity.

Interpretation: This is the first report of widespread rescue of dystrophin expression to therapeutic levels in the dog model of DMD. This study also provides a proof of concept for systemic multiexon-skipping therapy. Use of cocktails of morpholino, as shown here, allows broader application of this approach to a greater proportion of DMD patients (90%) and also offers the prospect of selecting deletions that optimize the functionality of the dystrophin protein.

Ann Neurol 2009;65:667–676

Duchenne muscular dystrophy (DMD) and its milder form, Becker muscular dystrophy (BMD), are caused by mutations in the *DMD* gene.[1] DMD is a progressive and fatal X-linked myopathy arising from the absence of functional dystrophin at the myofiber plasma membrane.[2] Most DMD mutations are caused by out-of-frame (frameshift) or nonsense gene mutations, whereas the majority of BMD mutations are in-frame, and thus compatible with production of a messenger RNA (mRNA) transcript that can be translated into a partly functional quasi-dystrophin (reading frame rule).[3] Some BMD patients with deletions as large as 33 exons (46% of the gene) can show little or no clinical symptoms, with only increased serum creatine kinase concentration.[4] This raises the possibility of using antisense-mediated removal of exons carrying nonsense mutations, or whose presence disrupts the open reading frame at the site of the mutation, so as to restore the translational reading frame and thus to convert DMD to a milder BMD phenotype.[5] Recently, intramuscular injection of 2′O-methylated phosphorothioate (2′O-MePs) has been shown to induce limited dystrophin expression in four DMD boys.[6] These studies, and extensive *mdx* mouse model systemic intravenous delivery reports, have rescued dystrophin expression by targeting a single exon. However, many DMD patients would require skipping of two or more exons to restore the reading frame. The ability to use cocktails of antisense oligonucleotides targeting multiple exons would permit design of quasi-dystrophin proteins that retain more functionality,[7] Finally, the use of cocktails could lead to FDA-approved mixtures that would successfully treat a large group of DMD patients with distinct but overlapping deletions. This might alleviate the problem

From the [1]Research Center for Genetic Medicine, Children's National Medical Center, Washington, DC; [2]McColl-Lockwood Laboratory for Muscular Dystrophy Research, Neuromuscular/Amyotrophic Lateral Sclerosis Center, Carolinas Medical Center, Charlotte, NC; and [3]Department of Molecular Therapy, National Institute of Neuroscience, National Center of Neurology and Psychiatry, Kodaira, Tokyo, Japan.

Address correspondence to Dr Hoffman, Research Center for Genetic Medicine, Children's National Medical Center, Department of Integrative Systems Biology, George Washington University School of Medicine, 111 Michigan Avenue NW, Washington, DC 20010. E-mail: ehoffman@cnmcresearch.org or Dr. Takeda, Department of Molecular Therapy National Institute of Neuroscience, National Center of Neurology and Psychiatry 4-1-1 Ogawa-higashi, Kodaiva, Tokyo, Japan. E-mail: takeda@ncnp.go.jp

Potential conflict of interest: Nothing to report.

Additional Supporting Information may be found in the online version of this article.

Received Jul 1, 2008, and in revised form Nov 29. Accepted for publication Dec 5, 2008.

Published in Wiley InterScience (www.interscience.wiley.com). DOI: 10.1002/ana.21627

of performing toxicology tests and FDA approvals for each individual antisense sequence; a formidable barrier to clinical application. Skipping of more than one exon could, theoretically, increase the applicability to some 90% of DMD patients[7,8] while aiming to produce the most functionally favorable dystrophin variants.[7]

The canine X-linked muscular dystrophy (CXMD) harbors a point mutation within the acceptor splice site of exon 7, leading to exclusion of exon 7 from the mRNA transcript.[9] We used the Beagle model here, the mutation of which originates from the Golden Retriever model, but which is less severely affected. At least two further exons (exons 6 and 8; Fig 1) must be skipped (multiexon skipping) to restore the open reading frame; therefore, it is more challenging to rescue dystrophic dogs with an exon-skipping strategy. Previously, McClorey and colleagues[10] showed transfection with antisense oligo targeting exons 6 and 8 restored reading frame of mRNA in cultured myotubes from dystrophic dogs *in vitro*. Here, we identified a phosphorodiamidate morpholino oligomer (PMO) cocktail that, using either intramuscular injection or systemic intravenous delivery, was not toxic, resulted in extensive dystrophin expression to therapeutic levels, and was associated with significant functional stabilization in dystrophic dogs *in vivo*.

Methods

Animals

CXMD-affected dogs and wild-type littermates from 2 months to 5 years old were used in this study[11] (see the Supplementary Table). Institutional animal care and use committee of National Center of Neurology and Psychiatry Japan approved all experiments using CXMD.

Antisense Sequences and Chemistries

We designed four antisense sequences to target exons 6 and 8 of the dog dystrophin mRNA as follows: Ex6A (GTTGATTGTCGGACCCAGCTCAGG), Ex6B (ACCTATGACTGTGGATGAGAGCGTT), Ex8A (CTTCCTGGATGGCTTCAATGCTCAC), and Ex8B (ACCTGTTGAGAATAGTGCATTTGAT). Sequences were designed to target exonic sites of exon 6 (Ex6A) and exon 8 (Ex8A), or exon/intron boundary between exon 6 and intron 6 (Ex6B), or exon 8 and intron 8 (Ex8B) (see Fig 1). Two donor-site sequences (Ex6B and Ex8B) were designed to target 23bp of exon and 2bp of intron. Sequences were synthesized using two different backbone chemistries: 2′O-MePs (Eurogentec Liège, Belgium), and morpholino (Gene-Tools, LLC Philomath, OR).[12] We determined these sites based on the exonic splicing enhancer motifs, GC contents, and secondary structures. We also avoided self/heterodimers. U (uracil) was used instead of T (thymidine) for the synthesis of 2′O-MePs oligos. A discussion and fig-

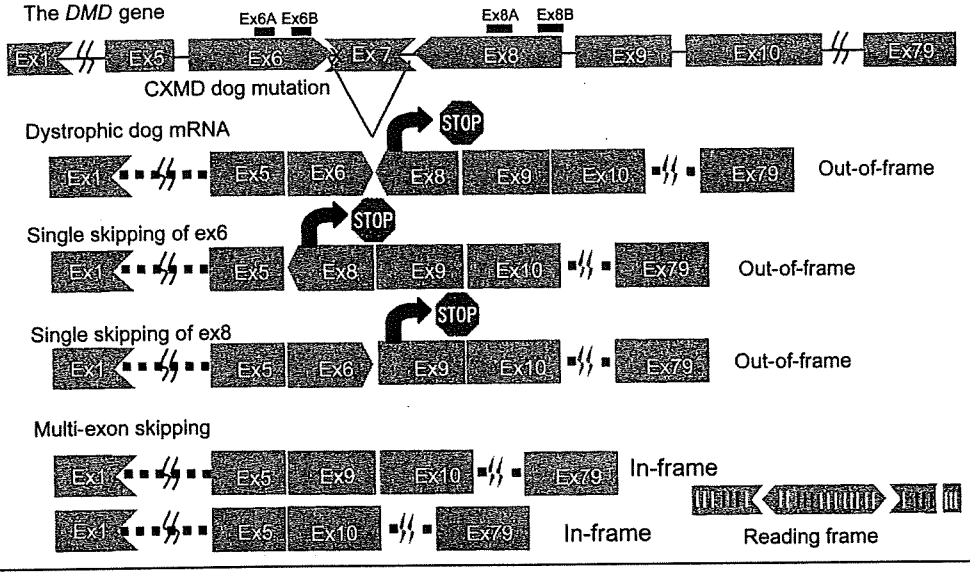

Fig 1. Mutation in canine X-linked muscular dystrophy (CXMD) and strategy for exon-skipping treatment. The dystrophic dog harbors a point mutation at splice site in intron 6, which leads to lack of exon 7 in messenger RNA. Single-exon skipping of exon 6 or 8 leads to out-of-frame products. Exclusion of at least two further exons (exons 6 and 8) is required to restore reading frame. Each extremity of the box represents the specific phasing of the exon. Left end of exons: 1: vertical lane (such as exon 6) means that the exon begins by the first nucleotide of a codon; 2) arrowhead toward left (such as exon 8) means that the exon begins by the second nucleotide of a codon; and 3) arrowhead toward right (such as exon 7) means that the exon begins by the third nucleotide of a codon. Right end of exons: 1) Vertical lane (such as exon 8) means that the exon ends by the last nucleotide of a codon; 2) arrowhead toward left (such as exon 1) means that the exon ends by the first nucleotide of a codon; and 3) arrowhead toward right (such as exon 6) means that the exon ends by the second nucleotide of a codon. DMD = Duchenne muscular dystrophy.

ure showing the alternative chemistries can be found in Yokota and colleagues' article.[13]

In Vitro Cell Transfections

Primary myoblast cells from neonatal CXMD dogs were obtained by standard methods using a preplating method.[14] Normal control (wild-type) or dystrophic (CXMD) myoblasts (1.5×10^5 cells) were cultured in growth medium containing F-10 growth media, 20% fetal calf serum, basic fibroblast growth factor (2.5ng/ml), penicillin (200U/ml), and streptomycin (200μg/ml) for 72 hours, followed by antisense oligonucleotide (2'O-MePs) administration (0.25–5μg/ml, 30–600nM) for 3 hours with lipofectin (Invitrogen, La Jolla, CA) following manufacturer's instructions (Antisense Oligo (AO)/lipofectin ratio = 1:2). The cells were cultured in differentiation medium containing Dulbecco's minimum essential medium with Horse Serum (HS) (2%), penicillin (200U/ml), and streptomycin (200μg/ml) for 4 to 5 days before analyses for RNA and protein. Morpholino antisense oligonucleotides carry no charge and cannot be transfected into cells efficiently, so only 2'O-MePs chemistry was utilized for *in vitro* studies.

Intramuscular Injections

Animals were anesthetized with thiopental sodium induction and maintained by isoflurane for all intramuscular injections and muscle biopsies. Skin was excised over the site of injection, muscle exposed, and the injection site marked with a suture in the muscle. Antisense oligonucleotides were delivered by intramuscular injection using 1ml saline bolus into the tibialis anterior or extensor carpi ulnaris (ECU) muscles using a 27-gauge needle. Antisense oligonucleotides were delivered either singly or in mixtures. Both 2'O-MePs and morpholino chemistries were tested. Muscle biopsies were obtained at 2 weeks after antisense injection.

Intravenous Systemic Delivery

Three dogs were treated and all were given an equimolar mixture of morpholinos Ex6A, Ex6B, and Ex8A at 32mg/ml each. Between 26 and 62ml was injected into the right saphenous vein using a 22-gauge indwelling catheter, leading to a cumulative (combined) dose of 120 to 200mg/kg per injection. Morpholinos were injected 5 to 11 times at weekly or biweekly intervals (see the Supplementary Table). Tissues were examined 2 weeks after the last injection.

Reverse Transcriptase Polymerase Chain Reaction and Complementary DNA Sequencing

Total RNA was extracted from myoblasts or frozen tissue sections using TRIzol (Invitrogen). Then reverse transcriptase polymerase chain reaction (RT-PCR) was performed on 200ng of total RNA for 35 cycles of amplification using One-Step RT-PCR kit (Qiagen, Chatsworth, CA) following manufacturer's instructions with 0.6mM of either an exon 5 (CTGACTCTTGGTTTGATTTGGA) or an exon 3/4 junction (GGCAAAAACTGCCAAAAGAA) forward primer. Reverse primers were either exon 10 (TGCTTCGGTCTCTGTCAATG) or exon 13 (TTCATCGACTACCACCACCA). The resulting PCR bands were extracted by using Gel extraction kit (Qiagen). BigDye Terminator v3.1 Cycle Sequencing Kit (Applied Biosystems) was used for complementary DNA sequencing with the same primers.

Hematoxylin and Eosin and Immunostaining

Eight micrometer cryosections were cut from flash-frozen muscle biopsies at an interval of every 200μm, then placed on poly-L-lysine–coated slides and air-dried. Anti-dystrophin rod (DYS-1) or C-terminal monoclonal Ab (DYS-2) (Novocastra Newcastle upon Tyne, UK) were used as primary antibodies. Rabbit anti-neuronal nitric oxide synthase (anti-nNOS) (Zymed Laboratory, San Francisco, CA) was used for nNOS staining. Alexa 468 or 594 (Invitrogen) was used as secondary antibody. 4',6-diamidino-2-phenylindole containing mounting agent (Invitrogen) was used for nuclear counterstaining (blue). The number of positive fibers for DYS-1 was counted and compared in sections where their biggest number of the positive fibers was as described previously.[15] Hematoxylin and eosin staining was performed with Harris hematoxylin and eosin solutions. Images were analyzed and quantified by using ImageJ software.[16]

Western Blotting Analysis

Muscle proteins from cryosections were extracted with lysis buffer containing 75mM Tris-HCl (pH 6.8), 10% sodium dodecyl sulfate, 10mM EDTA, and 5% 2-mercaptoethanol. Four to 40μg proteins were loaded onto precase 5% resolving sodium dodecyl sulfate polyacrylamide gel electrophoresis gels following manufacturer's instructions. The gels were transferred by semidry blotting (Bio-Rad Hercules, CA) at 240mA for 2 hours. DYS-2 (Novocastra) antibody against dystrophin, rabbit polyclonal antibody against α-sarcoglycan, and rabbit polyclonal antibody desmin were used as primary antibodies.[17] Horseradish peroxidase–conjugated anti–mouse or anti–rabbit goat immunoglobulin (Cedarlane Laboratories, Hornby, Ontario, Canada) was used as secondary antibodies. Enzyme chemiluminescence kit (GE Fairfield, CT) was used for the detection. Blots were analyzed by ImageJ software.

Blood Tests

Creatine kinase activity, blood counts, serum biochemistry, and toxicology test in canine serum were assayed with the Fuji Drychem system (Fuji Film Medical Co. Ltd, Tokyo, Japan) and Sysmex F-820 (Sysmex Corporation, Kobe, Japan) according to manufacturer's instruction.

Magnetic Resonance Imaging

For imaging studies, animals were anesthetized with thiopental sodium and maintained by isoflurane. We used a superconducting 3.0-Tesla magnetic resonance imaging (MRI) device (MAGNETOM Trio; Siemens Solutions, Erlanger, Germany) with an 18cm diameter/18cm length human extremity coil. The acquisition parameters for T2-weighted imaging were TR/TE = 4,000/85 milliseconds, slice thickness = 6mm, slice gap = 0mm, field of view = 18 × 18cm, matrix size = 256 × 256, and number of acquisitions = 3 during fast spin echo.

Functional Testing

Clinical evaluation of dogs was performed as described in our previous report.[18] Grading of clinical signs in CXMD dogs was as follows: gait disturbance: grade 1 = none, grade 2 = sitting with hind legs extended, grade 3 = bunny hops with hind legs, grade 4 = shuffling walk, and grade 5 = unable to walk; mobility disturbance: grade 1 = none, grade 2 = lying down more than normal, grade 3 = cannot jump on hind legs; grade 4 = increasing difficulty moving around, and grade 5 = unable to get up and move around; limb or temporal muscle atrophy: grade 1 = none, grade 2 = suspect hardness, grade 3 = can feel hardness or apparently thin, grade 4 = between grades 3 and 5, and grade 5 = extremely thin or hard; drooling: grade 1 = none, grade 2 = occasionally dribbles saliva when sitting, grade 3 = some drool when eating and drinking, grade 4 = strings of drool when eating or drinking, and grade 5 = continuous drool; macroglossia: grade 1 = none, grade 2 = slightly enlarged, grade 3 = extended outside dentition, grade 4 = enlarged and slightly thickened, and grade 5 = enlarged and thickened; dysphagia: grade 1 = none; grade 2 = takes time and effort in taking food, grade 3 = difficulty in taking food from plate, grade 4 = difficulty in chewing, swallowing, or drinking, and grade 5 = unable to eat.

For timed running tests, each dog was encouraged to run down a hallway (15m), and elapsed time was recorded. Single tests were done because dystrophic dogs tired rapidly.

Results

In Vitro Screening of Antisense Oligonucleotides in Dog Primary Myoblasts

The CXMD dog harbors a splice-site mutation of exon 7, leading to an out-of-frame mRNA transcript fusing exons 6 to 8 (see Fig 1). Both exons 6 and 8 must be excluded (skipped) from the mRNA to restore the reading frame. Four antisense oligonucleotides were designed against exons 6 and 8. Ex6A and Ex8A were designed to bind exonic splicing enhancers, and Ex6B and Ex8B were directed against the 5′ splice boundaries of each exon (see Fig 1). The four AOs were transfected as 2′O-MePs either singly or in mixture (cocktails; 5μg/ml each or 600nM each) into cultures of primary myoblasts isolated from the skeletal muscle of neonatal CXMD dogs. Four days after differentiation into myotubes, RNA was isolated and tested for specific exon skipping by RT-PCR. A cocktail of all 4 AOs produced a single 101bp band with 100% of RT-PCR product corresponding to a desired in-frame splice product of exons 5 to 10 (Fig 2A). It is of interest that exon 9, known to be an alternatively spliced exon in the dystrophin mRNA, was consistently skipped, although no antisense oligonucleotide was used against this exon (see Fig 2; see Supplemental Fig 1).[10] Each of the four sequences was also transfected individually, and either Ex6A or Ex6B successfully induced skipping as a single AO (100% in-frame product) (see Fig 2A). The precise skipping of exons was confirmed by complementary DNA sequencing (see Fig 2B). We found a dose–response relation where use of 30 and 60nM of either Ex6A or Ex6B induced multiexon skipping of exons 5 to 10, although with less efficiency and more intermediate out-of-frame products (see Supplemental Fig 1A). In contrast, the Ex8A AO alone induced skipping of mainly exons 8 and 9, an

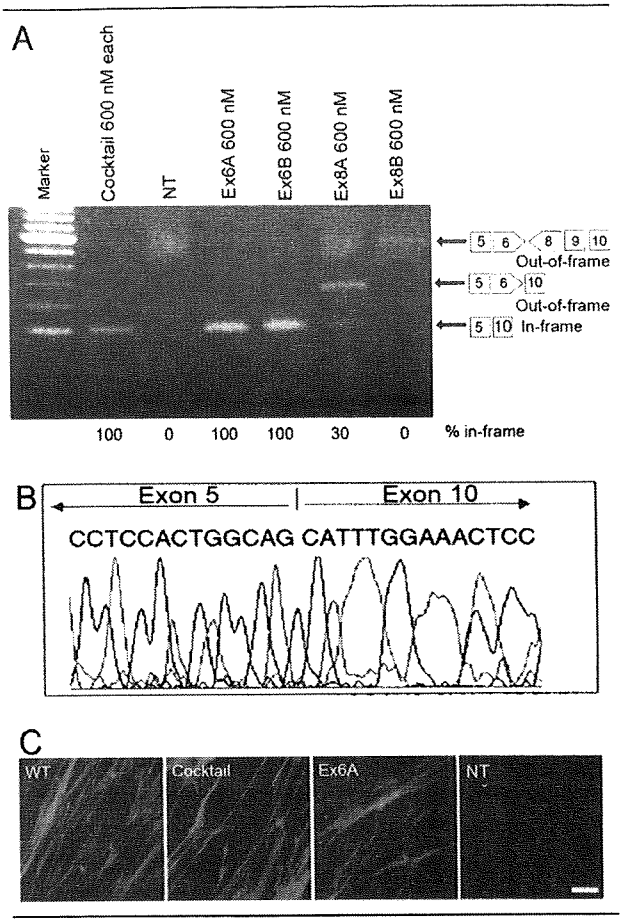

Fig 2. In vitro screening of antisense oligonucleotides and recovery of dystrophin expression by single antisense oligos in dog primary myoblasts. (A) Detection of exons 6 to 9 skipped in-frame products (101bp) using reverse transcriptase polymerase chain reaction (RT-PCR) at 4 days after the transduction of 5μg (600nM) each AOs of single (Ex6A or Ex6B) or cocktail AOs (Ex6A, Ex6B, Ex8A, and Ex8B) as indicated. A faint 585bp out-of-frame band is detected in Ex8B-treated myotubes. Nontreated myotubes (NT) show little RT-PCR product, likely because of nonsense-mediated decay. (B) Complementary DNA (cDNA) sequencing after antisense oligonucleotide treatment at 4 days after the transduction of Ex6A alone, showing the desired in-frame exons 5 to 10 skip. (C) Immunocytochemistry with dystrophin C-terminal antibody (Dys-2; red) and nuclear counterstaining (blue) for primary myotubes from canine X-linked muscular dystrophy (CXMD) cells at 4 days after transfection with cocktail or single antisense 2′O-methylated phosphorothioate (2′O-MePs) targeting exons 6 and 8 (5μg each/ml, or 600nM), nontreated wild-type (WT) cells, and CXMD cells. Scale bar = 50μm.

out-of-frame transcript, whereas the Ex8B AO induced no detectable exon skipping (see Fig 2A). Dystrophin protein production from in-frame mRNA was confirmed by immunocytochemistry using either the four-sequence cocktail or Ex6A alone (see Fig 2C).

We tested the same sequences in normal (wild-type) control Beagle cells (see Supplemental Fig 1B-C). When transfected into wild-type Beagle myoblasts, exon 9 was again routinely removed from the transcripts. The antiexon 8 AO pair excised exon 8, similar to dystrophic cells, whereas the exon 6–specific AO pair excised exon 6, as well as exon 9, but left exons 7 and 8 in place.

Efficient Skipping In Vivo Requires a Three-AO Cocktail

Given that Ex8B appeared ineffective by all *in vitro* assays, we did not continue with this sequence. Intramuscular injections were done using Ex6A alone, and equimolar mixtures of Ex6A, Ex6B, and Ex8A. Intramuscular injections into the tibialis anterior or ECU muscles of 0.5- to 5-year-old CXMD dogs were done for both 2'O-MePs and morpholino chemistries, at a dose of 0.12 to 1.2mg of each sequence (Fig 3; see Supplemental Fig 2). Biopsies were performed 2 weeks later at injection sites, marked by suture threads. Dystrophin-positive fibers were concentrated around the injection site, and the absolute number of dystrophin-positive fibers was counted in cross section.

In contrast with the skipping patterns observed with *in vitro* cell transfections, injection of Ex6A alone induced skipping of only exon 6 in experiments using either morpholinos or 2'O-MePs chemistries (see Fig 3; see Supplemental Fig 2). By contrast, the cocktail of Ex6A, Ex6B, and Ex8A induced robust dystrophin expression in a highly dose-dependent manner), with 1.2mg per each morpholino showing areas of complete dystrophin rescue, and high levels of dystrophin by immunohistochemical analysis and immunoblot (see Figs 3A, B, D; see Supplemental Fig 2). Intramuscular injections using the same cocktail with 2'O-MePs chemistry showed similar results, with greater dystrophin rescue using the three AO cocktail compared with Ex6A alone (see Fig 3C). Two pairwise combinations of Ex8A with either Ex6A or Ex6B were tested with morpholino chemistry, and neither combination proved as efficient as the three-sequence cocktail (see Fig 3B).

RT-PCR analyses of injected muscles showed that the Ex6A/Ex6B/Ex8A morpholino cocktail drives efficient skipping of exons 6 to 10 skipped products, with between 61 and 83% of RT-PCR products showing the desired in-frame product in the three muscles tested (see Fig 3D). Additional out-of-frame products were observed with Ex6A alone, and as a minority of products in the cocktail-treated muscles (see Fig 3D).

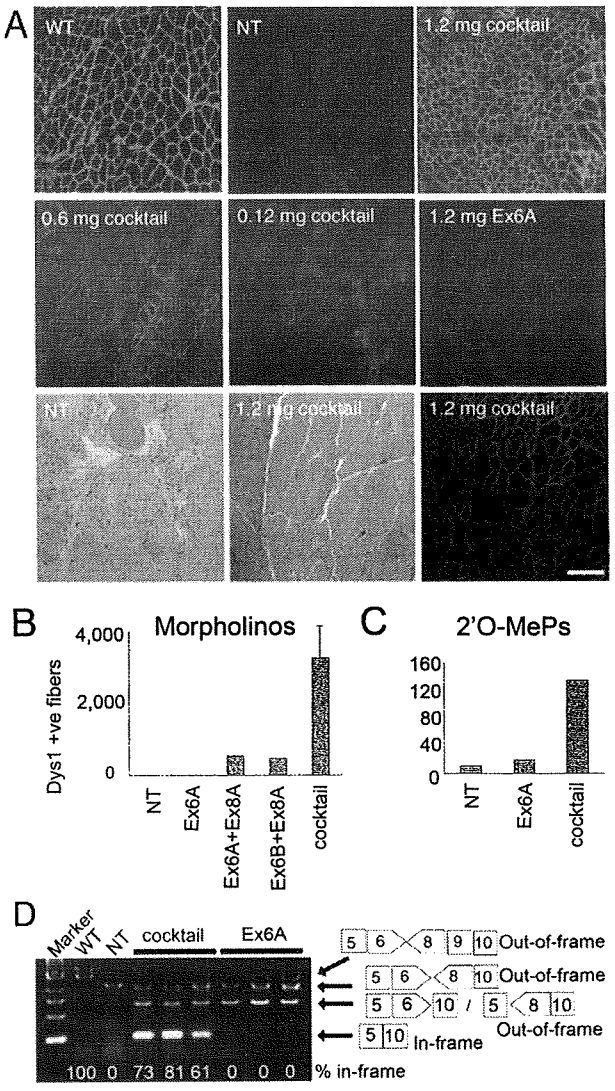

Fig 3. Recovery of dystrophin expression by in vivo intramuscular injection of a three-AO cocktail but not Ex6A alone. (A) Restoration of dystrophin expression in tibialis anterior (TA) at 14 days after single injection with 1.2mg Ex6A only, or cocktail containing 0.12mg each, 0.6mg each, or 1.2mg each of antisense morpholino Ex6A, Ex6B, and Ex8A are shown. Age-matched nontreated (NT) canine X-linked muscular dystrophy (CXMD) and wild-type (WT) dogs are shown as control animals. Hematoxylin and eosin (HE) staining at 14 days after 1.2mg each of the cocktail injection and age-matched nontreated control (NT), with consecutive cryosection stained with dystrophin (DYS-1) and 4',6-diamidino-2-phenylindole, show histological correction of the dystrophy. Bar = 100μm. (B, C) The number of DYS-1–positive fibers in TA or extensor carpi ulnaris (ECU) at 14 days after a single injection with cocktail (Ex6A+Ex6B+Ex8A), or indicated combinations, at 1.2mg each (morpholino; B), or 120μg each 2' O-methylated phosphorothioate (2' O-MePs) (C). Values are mean ± standard error of the mean. (D) RT-PCR analysis at 2 weeks after intramuscular injection of cocktail or Ex6A morpholino at 1.2mg each. The percentage of the in-frame exon 5 to 10 skip is shown under the gel image for treated muscle; normal control (WT) muscle shows the normal full-length in-frame transcript at the expected 100%.

Histological analyses of the muscle injected with the three-morpholino cocktail (1.2mg/each) showed significant histological improvement of the dystrophy, relative to uninjected muscle, (see Fig 3A; bottom panels).

By immunoblotting, intramuscular injection of the optimal cocktail induced dystrophin to 50% normal levels in a 2-year-old dog but only to 25% in a more clinically severe 5-year-old dog (see Supplemental Fig 2A). This result implies that the muscle quality influences the amount of dystrophin that can be produced.

Intravenous Systemic Delivery of a Morpholino Cocktail Induces Body-Wide Dystrophin Expression

AOs must be deliverable systemically to be of therapeutic value. Accordingly, we undertook intravenous infusion of the three morpholino-cocktail showing the most success in the intramuscular experiments (Ex6A, Ex6B, and Ex8A). Three CXMD dogs were studied using intravenous doses similar to that used in *mdx* mouse studies (30–40mg/kg per injection), with weekly or biweekly dosing. The first dog received 120mg/kg morpholinos (40mg/kg per each sequence) in weekly intravenous injections, with five doses over 5 weeks. The second dog was given the same dose 11 times at 2-week intervals over the course of 5.5 months. The third dog received a greater dose: 200mg/kg (66mg/kg of each morpholino) seven times at weekly intervals (see the Supplementary Table). All dogs were euthanized 2 weeks after the last injection, and multiple muscles were examined.

All skeletal muscles of each treated dog showed evidence of *de novo* dystrophin expression by immunofluorescence of cryosections, although the degree of rescue was variable (Fig 4A). Histopathology was markedly improved in regions showing high dystrophin expression (see Fig 4A). Immunoblotting confirmed expression up to approximately 50% of normal levels, but some muscles expressed only trace amounts (see Figs 4C, D). Dystrophin expression was also detected in cardiac muscles but, as in the *mdx* mouse,[19] less than in skeletal muscles and concentrated in small patches (see Fig 4A). Of the three dogs, the average dystrophin protein expression level was greatest in the dog given seven weekly doses of 200mg/kg PMO, with an average of 26% of normal dystrophin levels.

Selected muscles were studied for quantitative rescue of histopathology and for biochemical rescue of dystrophin-interacting proteins (dystrophin-associated glycoproteins and nNOS). A commonly utilized quantitative marker for muscle pathology is central nucleation of myofibers, where increased central nucleation is reflective of increased degeneration and regeneration. Quantitation of central nucleation in treated dogs compared with untreated littermates showed that intravenous antisense treatment reduced central nucleation in all five muscle groups examined (see Fig 4B).

Both nNOS and α-sarcoglycan are dystrophin-associated proteins that colocalize with dystrophin in normal muscle and are reduced in DMD muscle. nNOS immunofluorescence and α-sarcoglycan immunoblotting were done on a series of muscles from treated and control dogs. By immunoblot, α-sarcoglycan was seen to be increased in all muscles examined (Fig 5B). Likewise, nNOS was seen to relocalize to the membrane in dystrophin-positive regions in systemically treated dogs (see Fig 5A).

Muscle Imaging and Clinical Grading Scores Are Improved by Systemic Antisense Treatment

A global improvement in muscle pathology was further supported by the T2-weighted MRI examination (Fig 6). The high-intensity T2 signal, indicative of inflammation and increased water content, was diminished in PMO-treated dogs compared with pretreated and untreated control dogs in most muscles (see Fig 6).

Functional improvement of treated dogs was also assessed by a 15m timed running test and by a combined clinical grading score, as we have previously published.[18] Three dogs treated with intravenous morpholinos were compared with three untreated, at the ages of both 2 or 5 months (pretreatment) and 4 or 7 months (posttreatment) (Figs 7B, C). The untreated littermates became slower over the treatment time, whereas all treated dogs ran faster after treatment. The single dog treated at an older age with more advanced symptoms showed greater improvement relative to untreated littermates (see Fig 7B).

The combined clinical grading score similarly showed improvement or stabilization of disease progression after antisense treatment, relative to natural history controls (see Fig 7A). Videos documenting running ability of treated dogs and untreated littermates are available as supplemental data (see Supplemental Movies 1–5).

Serum creatine kinase was assessed before and after intravenous treatment, and compared with natural history controls (see Supplemental Fig 3). Although serum creatine kinase was variable, posttreatment creatine kinase levels were consistently less than natural history controls.

Intravenous High-Dose Morpholino Cocktail Shows No Evidence of Toxicity

No local inflammatory reactions or organ dysfunctions were recorded in the morpholino-treated dogs. Twice-weekly serum toxicology screens of the three systemically treated dogs showed no evidence of liver or kidney dysfunction (see Supplemental Fig 4). Levels of urea nitrogen, α-glutamyl transpeptidase, and creatinine all remained within the reference ranges. In addition, no significant changes were observed in amylase, total protein, total bilirubin, C-reactive protein, sodium, potas-

sium, or chloride. Growth of body weight was also within reference range in all treated dogs (data not shown).

Discussion

This is the first report of widespread induction of dystrophin expression to therapeutic levels in the dog model of DMD. Overall, our findings provide a promising message for DMD patients. Specifically, we show that intravenous morpholino antisense (PMOs) can generate body-wide production of functional dystrophin in a model clinically more severe than DMD, resulting in stabilization or improvement of the clinical disease. Beneficial effects were documented by histology, MRI, and functional tests (running and combined clinical grading scores).

We encountered some unexpected findings that raise important questions as to how to pursue this promising approach into human clinical trials. Clearly, the choice of specific antisense sequences is a crucial determinant of the ultimate success of targeted exon skipping. To date, specific AO sequences have been assessed for efficiency of exon skipping using cell-based experimental (*in vitro*) systems, with the optimal sequences then used for *in vivo* experiments. In studies presented here, antisense oligonucleotides directed against exon 6 were able to efficiently induce the desired exon 5 to 10 splicing *in vitro* but not *in vivo*. Our observations of discrepant outcomes for *ex vivo* and *in vivo* in the dystrophic dog tell us that we do not currently possess a reliable means of screening for sequences that induce efficient skipping of a particular exon in a particular mutational context. Data obtained from application of sequences as 2'O-MePs in primary myogenic cells or as PMOs incubated *ex vivo* with muscle fragments failed to predict the effects when PMO sequences were tested *in vivo*. The high percentage of in-frame products here might be related to nonsense-mediated decay of out-of-frame products or quality of RNA from cell culture; however, the *in vitro* experiments were consistent using three different concentrations (600, 60, and 30nM) with two different sequences (Ex6A and Ex6B). The results were confirmed by RT-PCR, immunohistochemistry, and complementary DNA sequences (see Fig 2; see Supplemental Fig 1). The *in vitro* effect of

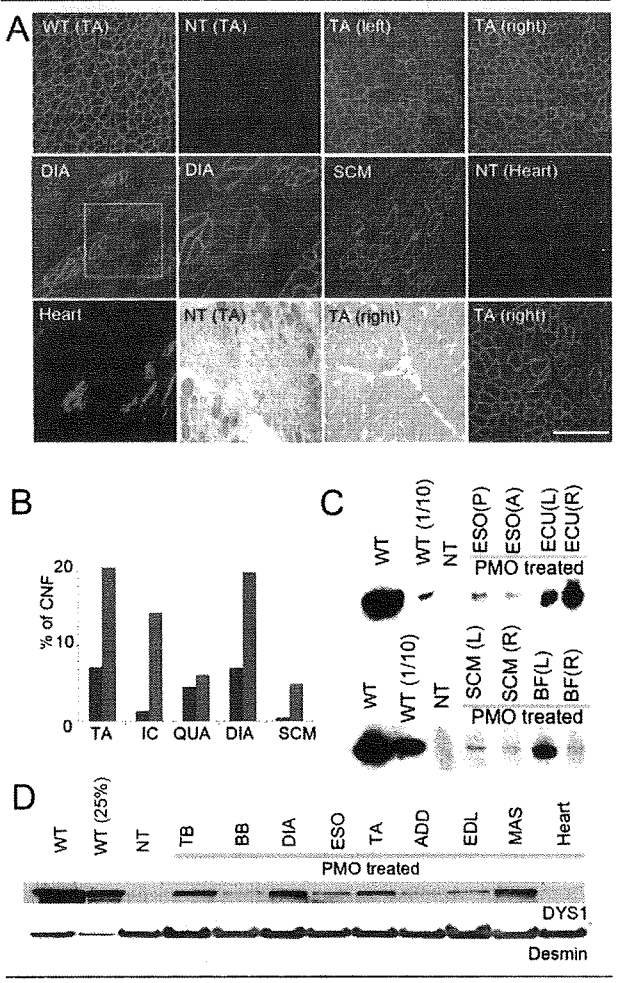

*Fig 4. Widespread dystrophin expression and improved histology by intravenous systemic delivery of cocktail morpholinos in canine X-linked muscular dystrophy (CXMD) dogs. (A) Dystrophin (DYS-1) staining and histology in bilateral tibialis anterior muscles (TA), diaphragm (DIA), sternocleidomastoid (SCM), and heart at 2 weeks after final injection after five weekly intravenous injections of 120mg/kg cocktail morpholinos containing Ex6A, Ex6B, and Ex8A (2001MA). Comparisons were made with TA from normal control animal (wild type [WT]) and from nontreated CXMD littermate (NT) tibialis anterior (TA) and heart. Intravenous morpholino treatment resulted in extensive, though variable, dystrophin production in multiple muscles, but with only limited evidence of rescue in heart (isolated cardiocytes). Paired dystrophin immunostaining and histology from treated dog (TA, bottom panels) showed improved histopathology relative to untreated littermate (NT TA) histology. Bars = 200μm, except for higher magnification picture of DIA and hearts (100μm). (B) Quantitation of centrally nucleated fibers (CNFs) in TA, intercostal (IC), quadriceps (QUA), diaphragm (DIA), and sternocleidomastoid (SCM) in treated dog (*blue bars; *2001MA) and untreated dog (red bars; 2008MA). (C) Western blotting analysis for detection of dystrophin at 2 weeks after final injection after 5 × weekly intravenous injections of 120mg/kg cocktail morpholinos containing Ex6A, Ex6B, and Ex8A (2001MA). Dystrophin rescue is variable with high expression in right extensor carpi ulnaris [ECU(R)] and left biceps femoris [BF(L)], and less in posterior [ESO(P)] or anterior esophagus [ESO(A)] and sternocleidomastoid (SCM). (D) Immunoblot analysis of dystrophin in intravenous morpholino-treated dog (2703MA; 7 × weekly dosing) and control animals (normal control [WT], nontreated [NT]). Desmin immunoblot is shown as a loading control. Dystrophin shows high levels (>25% control levels) in triceps brachii (TB), DIA, and masseter (MAS). ADD = adductor; BB = biceps brachii; EDL = extensor digitorum longus; MAS = masseter.*

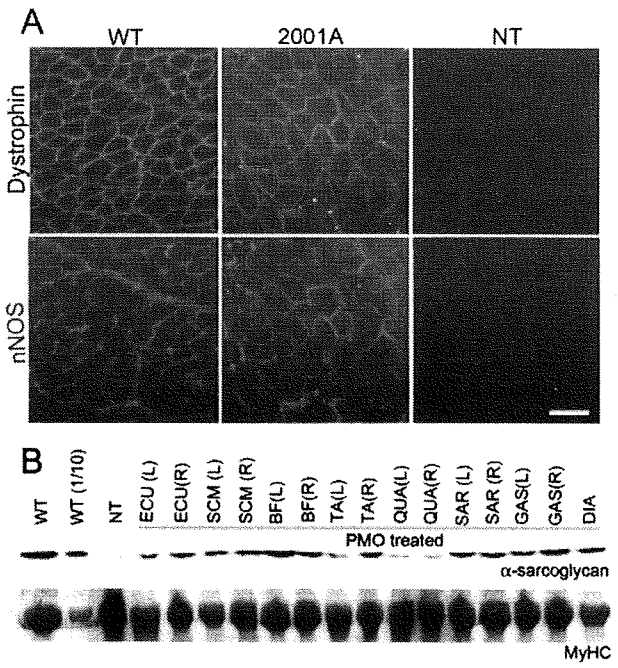

Fig 5. Recovery of localization and expression of dystrophin-associated proteins after systemic delivery of cocktail morpholinos to canine X-linked muscular dystrophy (CXMD) dogs. Neuronal nitric oxide synthase (nNOS) (A) and α-sarcoglycan (B) expression at 2 weeks after 5 × weekly 120mg/kg cocktail (2001MA) or 7 × weekly 200mg/kg cocktail morpholino injections (2703MA) to CXMD dogs. Recovery of nNOS expression at sarcolemma was observed by double immunofluorescence against dystrophin (DYS-1) and nNOS. Scale bar = 50μm. By immunoblot (B), α-sarcoglycan levels are increased in treated dog muscles, compared with untreated dystrophic controls (NT). Myosin heavy chain (MyHC) shown as a loading control. WT = wild-type normal control animals; WT(1/10) = wild-type (1/10 diluted samples, ie, 4μg loaded); NT = nontreated CXMD muscles (tibialis anterior); ECU = extensor carpi ulnaris; SCM = sternocleidomastoid; BF = biceps femoris; TA = tibialis anterior; QUA = quadriceps; SAR = sartorius; GAS = gastrocnemius; DIA = diaphragm; L = left side; R = right side.

the exon 6–specific sequence was, in addition, context dependent. For when transfected into wild-type Beagle myoblasts, the exon 8 AO pair again excised exons 8 and 9, whereas the exon 6–specific AO pair excised exons 6 and 9, leaving exons 7 and 8 in place (see Supplemental Fig 1). Thus, excision of exon 8 by the exon 6–specific sequences occurs only in the context of the mutant exon 7 splice site. Together, the differences between patterns of skipping *in vivo* versus *in vitro* and between wild-type versus mutant genotypes tell us that efficiency of skipping during transcription is dominated by variables other than the availability or otherwise of specific local sequence. Thus, it is prudent to consider testing of selected sequences in multiple systems with human dystrophin mRNA as the target before committing to a specific sequence for clinic trials.

We observed efficient skipping of exon 9, even though no antisense sequence targeted its removal in both wild-type and CXMD (see Figs 2 and 3), which is known as alternative splice site.[20] AOs targeting exon 8 have been reported to induce skipping of both exon 8 and 9 in human and in dog studies (see Figs 2 and 3).[10,21] It appears likely that the small size of intron 8 compared with intron 7 (1.1 vs 110Kb) predisposes to splicing of exon 8 to exon 9 before splicing to exon 7.

In the systemically treated dogs, we found widespread expression of dystrophin in all muscles analyzed but with considerable variation (see Fig 4). No difference in dystrophin expression between fiber types was evident

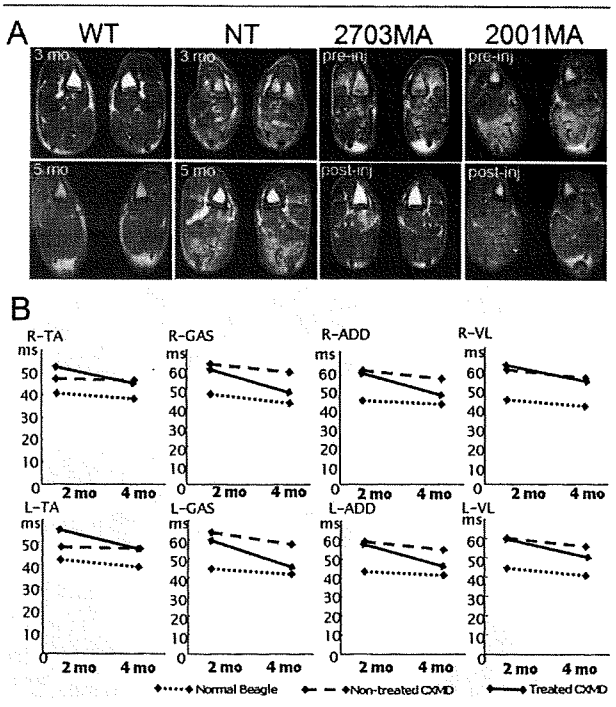

Fig 6. Amelioration of pathology and reduced inflammation signal in magnetic resonance imaging (MRI). T2-weighted MRI of hind legs at 1 week before initial injection (pre-inj) and at 2 weeks after final injection (post-inj) of 7 × weekly intravenous (IV) injection of 200mg/kg cocktail morpholinos (2703MA) or 5 × weekly IV injection of 120mg/kg cocktail morpholinos (2001MA). Age-matched untreated dogs (wild type [WT; normal control] and nontreated dystrophic control [NT]) are shown for comparison. (B) Changes of T2 value examined by MRI at 2 weeks after 7 × weekly 200mg/kg cocktail morpholino injections. Changes of T2 values in hind legs at 1 week before initial injection and at 2 weeks after final injection are shown. Intravenous morpholino treatment resulted in decreased T2 signal in all muscles examined. TA = tibialis anterior; GAS = gastrocnemius; ADD = adductor; VL = vastus lateralis. Dotted lines *represent normal Beagle;* dashed lines *represent nontreated canine X-linked muscular dystrophy (CXMD);* solid lines *represent treated CXMD.*